

# A Mutant Ataxin-3 Putative–Cleavage Fragment in Brains of Machado–Joseph Disease Patients and Transgenic Mice Is Cytotoxic above a Critical Concentration

Daniel Goti,<sup>1\*</sup> Scott M. Katzen,<sup>1\*</sup> Jesse Mez,<sup>1\*</sup> Noam Kurtis,<sup>1</sup> Jennifer Kiluk,<sup>1</sup> Lea Ben-Haiem,<sup>2</sup> Nancy A. Jenkins,<sup>3</sup> Neal G. Copeland,<sup>3</sup> Akira Kakizuka,<sup>4</sup> Alan H. Sharp,<sup>5</sup> Christopher A. Ross,<sup>6</sup> Peter R. Mouton,<sup>7</sup> and Veronica Colomer<sup>1</sup>

<sup>1</sup>Department of Psychiatry, Johns Hopkins University School of Medicine, Baltimore, Maryland 21287, <sup>2</sup>Institut de Génétique et de Biologie Moléculaire et Cellulaire, 67404 Illkirch Cedex, France, <sup>3</sup>Mouse Cancer Genetics Program, National Cancer Institute, Frederick Cancer Research and Development Center, Frederick, Maryland 21702, <sup>4</sup>Laboratory of Functional Biology, Kyoto University, Kyoto 606-8501, Japan, <sup>5</sup>Department of General Medical Sciences, Case Western Reserve University School of Medicine, Cleveland, Ohio 44106, <sup>6</sup>Division of Neurobiology, Department of Psychiatry, and Departments of Neurology and Neuroscience, Johns Hopkins University School of Medicine, Baltimore, Maryland 21205, and <sup>7</sup>Stereology Resource Center, Inc., Chester, Maryland 21619

Machado–Joseph disease (MJD) is an inherited neurodegenerative disorder caused by ataxin-3 with a polyglutamine expansion. It is proposed that a toxic cleavage fragment of mutant ataxin-3 alternatively spliced isoform mjd1a triggers neurodegeneration, although this fragment has not yet been detected in the brains of MJD patients or in animal models. We have now generated transgenic mice expressing human mutant (Q71) or normal (Q20) ataxin-3 mjd1a under the control of the mouse prion promoter. Q71 transgenic mice expressing mutant ataxin-3 mjd1a above a critical level developed a phenotype similar to MJD including progressive postural instability, gait and limb ataxia, weight loss, premature death, neuronal intranuclear inclusions, and decreased tyrosine hydroxylase-positive neurons in the substantia nigra (determined by unbiased stereology). Q20 transgenic mice had normal behavior and pathology. Brains from sick Q71 transgenic mice contained an abundant mutant ataxin-3 mjd1a putative–cleavage fragment (Fragment), which was scarce in normal Q71 transgenic mice. Reactivity of the Fragment with a panel of antibodies and comigration with truncations of mutant ataxin-3 revealed that it contained residues C terminal to amino acid 221 to include the polyglutamine expansion. A similar portion of mutant ataxin-3 mjd1a expressed in transfected neuroblastoma cells was toxic above a critical concentration. The Fragment was more abundant in two affected brain regions of MJD patients. Thus, we have developed a murine model for mutant ataxin-3 mjd1a toxicity and identified a putative–cleavage fragment of the disease protein in the brains of these transgenic mice and MJD patients that is cytotoxic above a critical concentration.

**Key words:** neurotoxicity; Machado–Joseph; spinocerebellar ataxia type 3; ataxin-3; mouse model; cleavage fragment

## Introduction

Machado–Joseph disease (MJD), also called spinocerebellar ataxia type 3 (SCA3), is in many countries the most common

cerebellar ataxia inherited in a dominant manner (Matilla et al., 1995; Schols et al., 1995; Durr et al., 1996; Silveira et al., 1998; Jardim et al., 2001). The signs and symptoms include progressive postural instability, gait and limb ataxia, weight loss, and, in severe cases, premature death (Fowler, 1984; Sudarsky and Coutinho, 1995). The pathology of MJD includes severe neuronal loss in the spinal cord and selective brain regions such as dentate nuclei (cerebellum), pontine nuclei (brainstem), substantia nigra (basal ganglia), and, to a lesser degree, cerebellar cortex (Fowler, 1984; Sudarsky and Coutinho, 1995; Durr et al., 1996). Brain regions such as the cerebral cortex are typically spared from severe neuronal demise (Fowler, 1984; Sudarsky and Coutinho, 1995; Durr et al., 1996). Intranuclear inclusions are detected in affected and spared neurons of MJD patients (Paulson et al., 1997b; Schmidt et al., 1998; Yamada et al., 2001).

MJD belongs to a group of hereditary and neurodegenerative disorders caused by a protein with a polyglutamine expansion (Orr, 2001). In MJD, mutant ataxin-3 has 56–84 consecutive glutamines, whereas normal ataxin-3 has 14–37 (Kawaguchi et al., 1994; Takiyama et al., 1997). Two mutant ataxin-3 isoforms

Received July 8, 2004; revised Sept. 12, 2004; accepted Sept. 13, 2004.

This work was supported by awards to V.C. including a donation from J. C. Giera, an award from the Ataxia MJD Research Project, American Heart Association (AHA) Minority Scientist Development Award 96-2308, AHA Established Investigator Grant 0140166N, and National Institute of Neurological Disorders and Stroke (NINDS) Grant NS42731. C.A.R. was supported by NINDS Grants NS16375 and NS38144. We especially thank Colomer laboratory technicians Dale Brown, for assistance with mouse behavior studies and maintenance of the transgenic mouse lines, and Dale Shin, for preparing some of the figures; Drs. David Borchelt, Gabrielle Schilling, and Mitra Cowan for advice during the generation of the transgenic mice; Dr. Borchelt for setting up the collaboration with N.A.J. and N.G.C.; Debbie Swing for performing the zygote injections; Dr. Mark Becher for assistance with the pathology of founder transgenic mice; Dr. Kimmo Hatanpaa for dissecting human brain; and Dr. Anthony Lanahan for advice on RT-PCR. We also thank Ellen Winslow for assistance in the preparation of figures, Michael McLwaine and Jim Durum for shooting the mouse photographs, and Mary Keyser, Jay Reda, and Missy McCurdy for budget administration.

\*D.G., S.M.K., and J.M. contributed equally to this work.

Correspondence should be addressed to Dr. Veronica Colomer, Department of Psychiatry, Johns Hopkins University School of Medicine, 600 North Wolfe Street, Meyer Research Building, Room 4-158, Baltimore, MD 21287. E-mail: vcolomer@jhu.edu.

DOI:10.1523/JNEUROSCI.2734-04.2004

Copyright © 2004 Society for Neuroscience 0270-6474/04/2410266-14\$15.00/0

resulting from alternative splicing (mjd1a and ataxin-3c) have been detected in the brains of MJD patients (Kawaguchi et al., 1994; Schmidt et al., 1998; Ichikawa et al., 2001). Although selective neuronal loss occurs in the brains of MJD patients, the levels of mutant ataxin-3 expression are similar throughout the brain (Nishiyama et al., 1996; Paulson et al., 1997a).

The mechanisms that cause selective neurodegeneration are poorly understood. Previous work using transgenic animals and transfected cells demonstrated that neuronal toxicity is caused by mutant ataxin-3 mjd1a truncations, to include the polyglutamine expansion, but not the full-length protein (Ikeda et al., 1996; Paulson et al., 1997b; Warrick et al., 1998; Yoshizawa et al., 2000; Hara et al., 2001). Thus, it was proposed that a mutant ataxin-3 mjd1a toxic cleavage fragment is released in affected but not spared neurons (Ikeda et al., 1996). The proteolytic fragment is proposed to be a product of caspase enzymes (Wellington et al., 1998; Berke et al., 2004). A similar hypothesis was proposed for other polyglutamine diseases (Goldberg et al., 1996). The mutant ataxin-3 mjd1a putative–cleavage fragment was identified in permanent clones of a transfected cell line (Yamamoto et al., 2001), although not in brain homogenates of MJD patients (Paulson et al., 1997a; Berke et al., 2004) or in transgenic mice (Cemal et al., 2002).

We have now generated and characterized transgenic mice expressing human mutant (Q71) or normal (Q20) ataxin-3 mjd1a under control of the mouse prion promoter. The Q71 animals expressing the transgenic protein above a critical level in the brain developed a severe abnormal phenotype similar to MJD. The Q20 transgenic mice were normal. In support of the hypothesis that pathogenesis in MJD stems from a mutant ataxin-3 mjd1a toxic cleavage fragment, we report the first identification and characterization of such a fragment in the brains of Q71 transgenic mice and MJD patients.

## Materials and Methods

### Human tissue

Fixed and frozen brain sections from two MJD cases, 1965 (male, 52 years old, 4 hr autolysis) and 2024 (male, 36 years old, 3.5 hr autolysis), and from normal controls, 2921 (24.5 hr autolysis) and 2519 (9.5 hr autolysis), were obtained from the National Neurological Research Specimen Bank (Los Angeles, CA). Brain sections from a third MJD case, 1704 (female, 60 years old, 21.5 hr autolysis), and normal individual 48,108 were obtained from Drs. Juan Troncoso and Kimmo Hatanpaa from the Department of Pathology, Johns Hopkins University School of Medicine. All MJD cases were diagnosed on the basis of abnormal signs and symptoms. Representative brain sections of all of these patients and normal individuals were stained with hematoxylin and eosin and analyzed by light microscopy. In the MJD cases, there was a dramatic reduction in the number of neurons in dentate nuclei of the cerebellum and the pigmented neurons in the substantia nigra compared with controls. The cerebellar cortex and frontal cortex of these MJD patients and control individuals were morphologically comparable.

### Transgenic mice

The isolation of the full-length human normal (Q20) or mutant (Q71) ataxin-3 mjd1a cDNAs has been described previously (Kawaguchi et al., 1994). These cDNAs were subcloned into our modified pCDNA3 vector (pCDNA3-NotI minus *XhoI*–*XhoI*). The *XhoI* inserts containing the human normal or mutant ataxin-3 cDNAs were subcloned next into the *XhoI* cloning site of the mouse prion promoter vector (MoPrP.Xho) (Borchelt et al., 1996). The correct insert orientation was determined by *SmaI* digestion. The isolation of the transgene plasmid DNA was done according to standard procedures (5 Prime → 3 Prime, Boulder, CO), except for eluting the DNA at 85°C. To confirm that these constructs were correct, they were transfected into human embryonic kidney 293 (HEK293) cells by means of the calcium phosphate procedure (Clontech,

Palo Alto, CA), and lysates of these cells were subjected to Western blot analysis. The transgene constructs were sequenced to confirm the presence of 20 or 71 CAG repeats in normal and mutant ataxin-3 cDNAs, respectively. The transgene constructs were next prepared for zygote injection essentially as described previously (Schilling et al., 1999). Briefly, they were digested with *NotI* and subjected to 0.7% low-melting point agarose (BioWhittaker, Walkersville, MD) gel electrophoresis. The largest digestion product was excised, treated with gelase (Epicenter Technologies, Madison, WI) to remove agarose, and further purified by phenol/chloroform extractions. Next, 2  $\mu$ g of this purified DNA in 200  $\mu$ l of water was centrifuged at  $\sim 178,000 \times g$  for 5 min at maximum speed in an Airfuge (Beckman, Palo Alto, CA). Supernatants were injected into the male pronucleus of fertilized oocytes from C57BL/6J  $\times$  C3H/HeJ mice, which were implanted into pseudopregnant mice. Founder transgenic mice were identified by a standard three-way PCR assay with mouse tail genomic DNA using two primers complementary to the prion gene and vector (Schilling et al., 1999) and a third primer corresponding to a sense human ataxin-3 cDNA sequence (MJD1669, 5'-GCTGGGCATGGTGGTGGGCAC-3') to generate a transgene-specific product of 200 bp.

### Footprint analysis

Footprint analysis was performed according to methodology described previously (Clark et al., 1997). Briefly, the hindfeet of the animals were dipped in Indian ink. The animals were placed on a 100  $\times$  10 cm strip of white paper lining a three-wall cardboard tunnel (90  $\times$  10  $\times$  10 cm) and encouraged to walk by gently pressing their tail. Three strips of paper with clear footprints were obtained for each animal.

### Rotarod test

The movement coordination of the mice was assessed with a Rotarod test as described previously (Clark et al., 1997; Schilling et al., 1999). Groups of six transgenic or nontransgenic mice of the same age and sex were placed on the rod of a Rotarod apparatus (Econometx; Columbus Instruments, Columbus, OH). The rod accelerated in 4 min from 4 to 40 rpm and remained at 40 rpm for the rest of the trial (acceleration, 1.50; slope, 2.50; sensitivity, 8.32). The time for each animal to fall off the rod was recorded. On four consecutive days, mice were subjected to four trials with at least 10 min of rest between trials. The data collected for each group of animals were represented in a box plot using KaleidaGraph (Synergy Software, Reading, PA).

### Grip strength measurement

The grip strength of forelimbs and hindlimbs was determined consecutively using a Grip Strength Meter with a triangular rod attachment (Columbus Instruments). Each mouse was held by the tail, and the limbs not subjected to the test were supported with, for example, a pencil. The mouse was lowered over the rod until it could easily grip the rod. The tail was then steadily and horizontally pulled away from the rod until the mouse released its grip, and the maximal force in pounds required for this to occur was recorded. Mice failing to grip the rod received a score of zero. On 1–3 consecutive days, each mouse was subjected to one to three trials per day with at least 5 min of rest between trials. Mice showing no ability to grasp the rod were subjected to the smaller number of trials. The data for each group of animals were represented by a box plot.

### Mouse activity test

The open-field activity was measured using a passive infrared activity monitor (Mini Mitter, Bend, OR). The monitor was suspended on a plastic frame over an uncovered empty mouse cage. Mice were placed alone in the cage and monitored for a period of 5 min. In a pilot experiment using three sick and three wild-type mice, we established that 5 min of testing once per day on 3 consecutive days was sufficient to demonstrate group differences in activity levels. Several hour measurements showed more dramatic differences, but additional tests of this length were impractical with only one monitor. The data collected for each group of animals were represented in a box plot.

### Righting reflex test

Righting reflex was measured by rotating the tail to place the mouse on its back. Mice that resisted this rotation received a score of zero. If the mouse

did not resist, the time it took the mouse to right itself to a normal posture was recorded. Each mouse was subjected to three consecutive trials per day on 3 consecutive days. The data collected for each group of animals were represented in a box plot.

#### *Ataxin-3 antibodies*

Rabbit polyclonal antisera to full-length His-tagged ataxin-3 lacking amino acids 64–78 was a gift from Dr. Henry Paulson (Department of Neurology, University of Iowa College of Medicine, Iowa City, IA) (Paulson et al., 1997a). Mouse monoclonal antibodies 2B6 and 1H9 were a gift from Dr. Yvon Trotter (Institut de Génétique et de Biologie Moléculaire et Cellulaire, Illkirch, France) (Trottier et al., 1998).

Polyclonal antibodies 144 and 146 were prepared as follows: Antibody 144 was developed against peptide MESIFHEKQEGSLC (peptide named MJD1) corresponding to ataxin-3 amino acids 1–14 of ataxin-3 mjd1a. The peptide was coupled through its cysteine residue to thyroglobulin and albumin, using sulfo-SMCC [sulfo-succinimidyl 4-(*N*-maleimidomethyl)-cyclohexane-1-carboxylate] cross-linking reagent (Pierce, Rockford, IL). The coupling procedure followed was described previously (Harlow and Lane, 1988; Sharp et al., 1995). Antibody 146 was developed against peptide LSGQSSHP CERPA (MJD 320) corresponding to ataxin-3 mjd1a amino acids 320–334. The peptide was coupled to bovine thyroglobulin and BSA through its N-terminus amino group using 0.1% glutaraldehyde, as described previously (Harlow and Lane, 1988; Sharp et al., 1995). Rabbits were immunized with peptide–thyroglobulin and boosted with peptide–albumin at Cocalico Biologicals (Reamstown, PA). Glutathione S-transferase (GST) proteins were prepared essentially as described by the manufacturer (Amersham Biosciences, Piscataway, NJ) using pGEX4T2 constructs encoding ataxin-3 amino acids 1–296 (to pre-adsorb sera 146 and purify sera 144) and 242–360 (to pre-adsorb sera 144 and purify sera 146). The GST proteins were coupled to cyanogen bromide-activated Sepharose 4B as described by the manufacturer (Amersham Biosciences, Piscataway, NJ) and used to purify the sera by standard affinity chromatography eluting with 100 mM glycine–HCl, pH 2.5, and neutralizing the fractions with 200 mM Tris, pH 8. The purified antibodies were dialyzed extensively against HEPES-buffered saline, pH 8, aliquoted, and frozen.

#### *Ataxin-3 epitopes recognized by monoclonal antibodies 1H9 or 2B6*

Monoclonal antibodies 2B6 and 1H9 were previously determined to bind ataxin-3 peptides 196-LAQLKEQRVHKTDLERMLEANDGS-219 and 214-EANDGSGMLDEDEEDLQRAL-233, respectively (Trottier et al., 1998). To define the epitopes recognized by these antibodies, four different tests were used following procedures described previously: dot blot, ELISA, competitive Western blot, and immunofluorescence (Trottier et al., 1998). In brief, dot blot and ELISA were performed by binding increasing concentrations of peptides with overlapping sequences to nitrocellulose or plastic, respectively, before immunodetection with each antibody. Competitive Western blot and immunofluorescence of transfected COS cells or human lymphoblasts expressing ataxin-3 were performed using the antibodies preincubated with different peptides with overlapping sequences. The seminal epitope recognized by antibody 1H9 was localized to sequence MLDE by dot blot, competitive Western blot (see Fig. 6C), ELISA, and competitive immunofluorescence (data not shown). The epitope recognized by the 2B6 antibody was localized to 202-QRVHKTDLERMML-213 by dot blot and ELISA but to 202-QRVHKTDLERMLEANDGS-219 by competitive Western blot and immunofluorescence (data not shown).

#### *Mouse perfusion*

Mice were perfused according to a standard procedure (Schilling et al., 1999). Briefly, the animals were anesthetized by inhalation of isoflurane (Minrad, Buffalo, NY) and subsequent intraperitoneal injection of 5 mg/0.1 ml pentobarbital sodium (Abbott Laboratories, North Chicago, IL) before perfusion with ice-cold PBS for 1–2 min, followed by ice-cold PLP (2% paraformaldehyde, 75 mM DL-lysine, and 10 mM sodium periodate in PBS, pH 7.2–7.4) for 8 min. After perfusion, the brain and spinal cord were removed, postfixed in PLP overnight at 4°C, and then transferred to PBS.

#### *Immunohistochemistry*

Mouse brains were cut in half along the midsagittal plane. These blocks, spinal cord, and human brain blocks were processed and embedded in paraffin by the histology core facility at Johns Hopkins Medical Institution. Slides with paraffin sections 6  $\mu$ m thick for mouse brain or spinal cord and 10  $\mu$ m for human brain were steamed for antigen retrieval and then incubated with ataxin-3 antibody 144 (at 1:10 or 1:40) or ataxin-3 antibody 146 (at 1:100). A universal secondary antibody (anti-rabbit and -mouse) was applied, followed by ABC coupled to horseradish peroxidase (HRP; Dako, Carpinteria, CA) and DAB substrate (Vector Laboratories, Burlingame, CA). The slides were counterstained with hematoxylin according to standard procedures and analyzed under an Eclipse E400 (Nikon, Tokyo, Japan) microscope using visible light and a 100 $\times$  objective. Photographs were taken using ND4 and ND8 filters and Ektachrome 100plus photographic film. A 50  $\mu$ m bar under the 100 $\times$  objective was used for assessing magnification.

#### *Stereology*

Groups of four to five transgenic mice of the same sex and age were perfused as described above. Whole brain was paraffin embedded, and 50  $\mu$ m sections were cut through the dentate nucleus (also known as lateral nucleus) from bregma –5.68 to –6.36 and tyrosine hydroxylase (TH)-positive neurons in the substantia nigra (pars compacta) from bregma –2.54 to –3.88 (Paxinos and Franklin, 2001). A systematic-random series of 8–12 sections of each brain region were used. The substantia nigra sections were immunostained with a rabbit antibody to TH (Chemicon, Temecula, CA) at a 1:500 dilution, biotinylated goat anti-rabbit secondary antibody, streptavidin–HRP (Vector Laboratories), and DAB (Sigma, St. Louis, MO). These sections were counterstained, and the dentate nuclei slides were stained with cresyl violet (Nissl stain) and coverslipped. The total number of Nissl-stained neurons in dentate nuclei and TH-positive neurons in the substantia nigra were counted using the optical fractionator technique with assistance from the computerized stereology system (Stereologer, Alexandria, VA), as detailed previously (Mouton et al., 2002). Statistical analyses including ANOVA and power analysis were done using JMP software (SAS Institute, Cary, NC). Neurons in dentate nuclei were easily distinguishable from glial cells on the basis of size and morphology. The neurons in the substantia nigra are heterogeneous in size and difficult to distinguish from glial cells without immunostaining. TH is a marker for dopaminergic neurons (Greenfield et al., 2002), although a reduced number of positive cells could indicate cell death or a decrease in TH expression or immunoreactivity.

#### *Western blot analysis of brain tissue*

Brain tissue was homogenized in cold 0.1 M Tris–HCl, pH 7.5, 0.1 M EDTA, and a mixture of protease inhibitors (Complete; Roche, Indianapolis, IN). Protein concentrations were determined using a Coomassie protein assay (Pierce), and samples were prepared in standard SDS-PAGE sample buffer at a final concentration of 2.8–3.6 mg/ml. Samples were sonicated for 10 sec, heated for 3 min at 100°C, and microfuged for 10 sec before loading 20  $\mu$ l per sample on polyacrylamide minigels (3–16% gradient; Bio-Rad, Hercules, CA) or 100  $\mu$ l per sample on large gels (3–16% gradient, 1.5 mm thick, Hoefer SE 600; Amersham Biosciences, San Francisco, CA). After SDS-PAGE, proteins were transferred electrophoretically onto nitrocellulose membranes with a 0.2  $\mu$ m pore size (Schleicher & Schuell, Keene, NH) in buffer containing Tris–glycine and 10% methanol for 1–3 hr (300 mA constant amperage for minigels) or 4 hr (400 mA constant amperage for large gels). The stacking gel was left on during transfer, and 0.05% SDS was added to transfer buffer when necessary to detect aggregates. The blots were blocked in PBS–5% dry milk before incubation overnight at 4°C with the primary antibody. Polyclonal antibody to full-length ataxin-3 was used at 1:2000, polyclonal antibody 146 was used at 1:14, polyclonal antibody 144 was used at 1:10, monoclonal antibody 2B6 or 1H9 was used at 1:2000, monoclonal antibody 1C2 (Chemicon) was used at 1:250, and a monoclonal antibody to glyceraldehyde-3-phosphate dehydrogenase (GAPDH; Advanced Immunochemical, Long Beach, CA) was used at ~1:400; polyclonal antibody to TBP (TATA-binding protein; QED Biosciences, San Diego, CA) was used at 1:300. Bound primary antibodies were visualized with goat anti-mouse or goat anti-rabbit HRP-conjugated secondary antibodies at

1:10,000 (Boehringer Mannheim, Indianapolis, IN), chemiluminescent substrate (Supersignal; Pierce), and exposure on autoradiography film. Alternatively, when quantitations of the ataxin-3-immunostained bands were needed, the blot was developed using  $^{125}\text{I}$  protein A (PerkinElmer Life Sciences, Boston, MA) at 1:1000 and a PhosphorImager screen (Storm; Molecular Dynamics, Sunnyvale, CA). We quantitated the PhosphorImager units in bands of interest in two or three similar blots using ImageQuant software (Molecular Dynamics), averaged the values, and calculated SDs.

#### Subcellular fractionation

Cytoplasmic and purified nuclear fractions of mouse brain or human brain sections were prepared according to procedures described previously (Israel and Whittaker, 1965; Blobel and Potter, 1966) with modifications. Briefly, 2.5 ml of homogenization buffer (0.32 M sucrose, 25 mM KCl, 5 mM  $\text{MgCl}_2$ , 50 mM triethanolamine, pH 7.4) with protease inhibitors (Complete, EDTA-free; Boehringer Mannheim) was added to an ice-cold Teflon pestle tissue homogenizer. Frozen brain tissue (300 mg or half of a mouse brain cut sagittally) was added to the homogenization buffer and subjected to nine strokes of the Teflon pestle driven at 900 rpm. The homogenate was transferred through cheesecloth into two 2 ml tubes (PGC Scientific, Frederick, MD) and centrifuged at  $770 \times g$  for 10 min at 4°C. The supernatants were removed and pooled (S1). The pellet was vortexed gently in the original volume of homogenization buffer and again centrifuged at  $770 \times g$  for 10 min at 4°C. The pellets were gently vortexed in 250  $\mu\text{l}$  of homogenization buffer per tube and pooled, and 1 ml of homogenization buffer containing 24% Ficoll was added to the bottom of the tube. The samples were centrifuged at  $10,600 \times g$  for 40 min at 4°C. The pellet was gently vortexed in 200  $\mu\text{l}$  of homogenization buffer. Then 200  $\mu\text{l}$  of homogenization buffer with 1% Triton X-100 was added, mixed by gentle inversion, and incubated for 20 min on ice. The sample was centrifuged at  $800 \times g$  for 10 min, and the pellet (P) was resuspended in 100–200  $\mu\text{l}$  of homogenization buffer. Equal amounts of protein for S1 and P were subjected to SDS-PAGE and Western blotting.

#### Reverse transcriptase-PCR assay

Wild-type or transgenic mouse brain poly(A<sup>+</sup>) mRNA was isolated with the use of an Oligotex Direct mRNA kit (Qiagen, Hilden, Germany) according to the manufacturer's protocol using 150–200 mg of frozen brain. The sequence of the primers used for PCR amplification was based on the published ataxin-3 mjd1a sequence (Kawaguchi et al., 1994): MJD13 sense, 5'-CCGTTGGCTCCAGACAAAATA-3'; MJD884 sense, 5'-GAAGAGACGAGAAGCCTACT-3'; MJD1713x antisense, 5'-GGAGT-TCAATGGCACAATC-3'. The PCR (MJ Research, Watertown, MA) settings were 96°C for 1 min, 60°C for 45 sec, and 70°C for 1 min, for 35 cycles. Reaction mixtures were analyzed using a 1.2% agarose gel containing ethidium bromide.

#### Generation of cDNAs encoding truncated ataxin-3

The full-length human normal (Q20) or mutant (Q71) ataxin-3 mjd1a cDNAs were subcloned into the *Bam*HI–*Eco*RV cloning site of pcDNA3 vector (Invitrogen, Carlsbad, CA). These constructs were subjected to PCR using a high-fidelity polymerase, platinum *Pfx*-DNA polymerase (Invitrogen). The oligonucleotides corresponding to the sense ataxin-3 cDNA sequences with a *Bam*HI restriction site and an initiation codon were 5'-GGCGGGATCCATGGAGGAGGATTTGCAGAGGG-3' for constructs Q20 $\Delta$ N225 and Q71N $\Delta$ 225, 5'-CGGCGGATCCATGTGCGAAGCTGACCAACTCCT-3' for constructs Q20 $\Delta$ N171 and Q71 $\Delta$ N171, or 5'-CGGCGGATCCATGACATATCTTGCACCTTTTCTTG-3' for constructs Q20 $\Delta$ N145 and Q71 $\Delta$ N145. The antisense primer contained the stop codon from the ataxin-3 cDNA and an *Eco*RV restriction site and was 5'-CGGCGATATCTTATGTTCAGATAAAGTGTGAAG-3'. The PCR settings were 94°C for 5 min and 32 cycles of 94°C for 15 sec, 55°C for 30 sec, and 68°C for 1 min. The PCR products were subcloned into the pcDNA3 vector at cloning sites *Bam*HI–*Eco*RV and sequenced (by the core facility at Johns Hopkins Medical Institution).

#### Neuro-2a cells: transfection and Western blot analysis

The transfections were done in triplicate in a mouse neuroblastoma cell line, Neuro-2a, cultured with complete medium  $\alpha$ -MEM Glutamax (In-

vitrogen) with 100 U/ml penicillin, 100 U/ml streptomycin, and 10% fetal calf serum. For each well of cells, 4  $\mu\text{g}$  of total plasmid DNA containing 0.2  $\mu\text{g}$  of luciferase plasmid (pRL-SV40 Renilla luciferase reporter vector; Promega, Madison, WI) and pcDNA3 vector or construct were precipitated with calcium phosphate for 20 min, according to the recommendations of the manufacturer (CalPhos Mammalian Transfection kit; BD Biosciences Clontech), and added to each well of cells. Four hours after transfection, the complete medium was replaced with fresh medium supplemented with retinoic acid at a final concentration of 20  $\mu\text{M}$  (Sigma-Aldrich, St. Louis, MO). Forty-eight hours after transfection, cells were harvested in ice-cold lysis buffer [Tris 10 mM, pH 8, containing 1 mM EDTA with protease inhibitors (Complete; Roche)]. After sonication, cell lysates were stored at  $-80^\circ\text{C}$  until used. Equal amounts of protein in each sample (0.8 mg/ml) were prepared in standard SDS-PAGE sample buffer with 20 mM  $\beta$ -mercaptoethanol and boiled for 3 min. Eighty microliters of sample were loaded per well in a large gel (see above). Proteins were transferred onto a nitrocellulose membrane in transfer buffer with 0.1% SDS for 2.5 hr (400 mA constant amperage).

#### Cytotoxicity assays

The Renilla luciferase assay kit was used according to the manufacturer's recommendations (Promega). In brief, 50  $\mu\text{l}$  of cell lysate (see above) was mixed with 500  $\mu\text{l}$  of lysis buffer (supplied with the kit). Immediately before inserting the vial in the luminometer, 20  $\mu\text{l}$  of cell lysate was mixed with 100  $\mu\text{l}$  of reaction buffer (supplied with the kit) by flicking the vial, and light emission was measured with a luminometer (TD-20E; Turner BioSystems, Sunnyvale, CA). The lactate dehydrogenase (LDH) release assay kit was used according to the manufacturer's recommendations (CytoTox96 Non-Radioactive Cytotoxicity assay; Promega).

## Results

### Generation of transgenic mice

We subcloned the cDNAs that code for human normal (Q20) or mutant (Q71) ataxin-3 mjd1a into a vector containing the mouse prion promoter and used these constructs to generate transgenic mice. The transgenic mice were identified by a standard PCR assay using mouse tail genomic DNA.

Of a total of 28 Q71 founders, representative ones being listed (supplemental material, available at [www.jneurosci.org](http://www.jneurosci.org)), three were used to develop heterozygous lines Q71-A, Q71-B, and Q71-C. Lines Q71-B and Q71-C were inbred to generate homozygotes, which were infertile but could be continuously generated from heterozygous parents. Two of a total of 25 Q20 founders were used to develop heterozygous lines Q20-A and Q20-B. The Q71 or Q20 transgenic construct in the corresponding heterozygous lines had a stable transmission in multiple generations with a predictive frequency of  $\sim 50\%$ .

Here, we include the data on Q71-B and Q71-C (heterozygotes and homozygotes) and Q20-A (heterozygous) transgenic mice that are representative of results obtained with the rest of the transgenic mice (supplemental material, available at [www.jneurosci.org](http://www.jneurosci.org)).

### Transgene expression

We established transgene expression in the brains of the transgenic mice by Western blotting with different ataxin-3 antibodies (Fig. 1). Q20-A and Q20-B transgenic mouse brains, like human cerebellum, had ataxin-3 of  $\sim 44$  kDa (Fig. 1, left blot). The two faint and higher-molecular-weight bands that were revealed in all samples by antibody 146 were nonspecific bands. In the brains of Q71-B homozygotes and heterozygotes, we detected human mutant ataxin-3 of  $\sim 58$ –64 kDa (Fig. 1, left blot). In a better resolving gel, mutant ataxin-3 appeared as a doublet in all Q71 transgenic mice (Fig. 1, right blot), but the top band was visible in some samples on a longer exposure of the blot (data not shown). Human mutant but not normal ataxin-3 was revealed with monoclonal antibody 1C2 (Fig. 1, middle blot), which preferen-

tially recognizes expanded polyglutamines (Trottier et al., 1995). Human mutant ataxin-3 expressed in HEK293 transfected cells and transgenic mouse brain comigrated (Fig. 1, middle blot). Together, the results indicated that the human normal and mutant ataxin-3 mjd1a expressed in mice had the expected size.

The level of transgene expression in the brains of Q20-A animals was higher than in Q71-B homozygotes (Fig. 1, left blot), indicating that the abnormal phenotype observed in Q71-B homozygotes but not in Q20 transgenic mice (described below) did not arise from generic toxicity caused by high transgene expression levels.

Murine ataxin-3 (~43 kDa) was detected readily with an antibody to full-length ataxin-3 (Fig. 1, right blot) but poorly by antibody 146 (Fig. 1, left blot) because the latter bound to a human ataxin-3 sequence with only 46% identity with murine ataxin-3. Mutant ataxin-3 and murine ataxin-3 were quantitated on three similar blots revealed with antibody to full-length mutant ataxin-3 (including the right blot in Fig. 1), and the average ratio and SD were calculated (Fig. 1, right blot). Increased transgene expression levels tended to correlate with a younger age at death (described below), an indication that the abnormal phenotype was determined by the transgenic protein rather than by genes altered at the transgene integration site.

### Appearance and behavior

At the onset of the abnormal phenotype, Q71-B homozygotes (2–4 months of age) and Q71-C homozygotes (2–3 months of age) had a tremor, groomed excessively, had the beginning of abnormal posture (hunchback), had ataxic limbs (transiently clutched paws and uncoordinated extension of their limbs) (Fig. 2A), and had lateral body displacement while trying to climb a cage wall. At a later stage, Q71-B homozygotes (4–8 months of age) and Q71-C homozygotes (3–5 months of age) exhibited tremor, pronounced abnormal posture (hunchback with low pelvic elevation and muscle wasting), ataxic limbs (permanently clutched paws and uncoordinated extended limbs) (Fig. 2A), low toe-pinch response, and occasional seizures. Q71-B heterozygotes, Q71-C heterozygotes, and Q20-A transgenic mice were indistinguishable in appearance and behavior from wild-type mice until they were killed at 15 months of age.

Q71 homozygotes developed a progressive unsteady gait as documented by footprint analysis (Fig. 2B). The Q71-B and Q71-C heterozygotes and the Q20-A transgenic mice, like wild-type mice, maintained a normal footprint pattern until they were killed at 15 months of age (Fig. 2B).

Q71-B and Q71-C homozygotes developed progressively impaired grip strength by forelimbs and hindlimbs (Fig. 3). At similar early ages, these animals failed to remain on an accelerating rod (rotarod) (Fig. 3), possibly because of their weak grip strength. They had a progressively deteriorating righting reflex, open-field activity, and body weight (40–60% weight loss at moribund stage) (Fig. 3). Like wild-type mice, Q20-A, Q71-B, and Q71-C heterozygotes did not develop these abnormal behaviors or weight loss (Fig. 3).

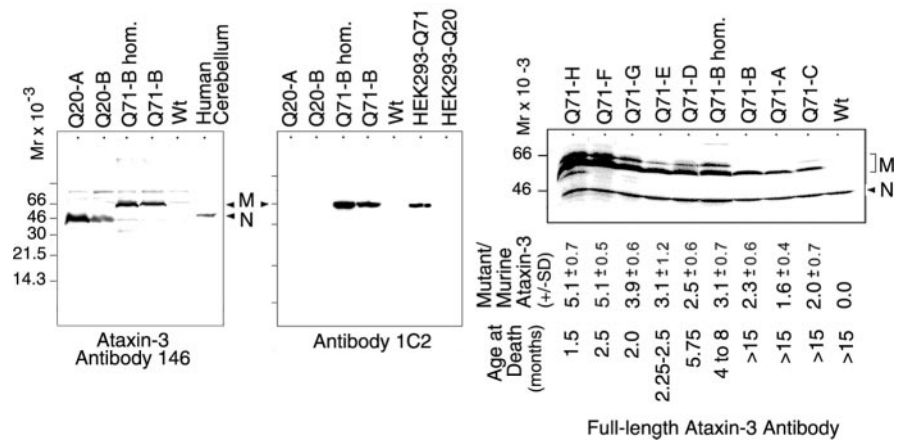


**Figure 1.** Transgene expression in the Q71 and Q20 transgenic mouse brain. Western blots of brain homogenates from the indicated transgenic mice [all heterozygous, except for Q71-B homozygotes (hom.)] or wild-type mice (Wt), human cerebellum, or lysates of transfected HEK293 cells expressing the MoPrP constructs (Q71 or Q20) are shown. The same amount of protein was analyzed per sample. The blots were revealed with the indicated ataxin-3 antibodies or antibody 1C2, which preferentially recognizes expanded polyglutamine repeats. The relative migration ( $M_r$ ) of each molecular weight standard used is indicated. Human mutant ataxin-3 (M) and human or murine normal ataxin-3 (N) are highlighted. The ratio of human mutant over murine ataxin-3 PhosphorImager units is shown under one blot. The results are the average of the values obtained in three similar blots and the corresponding SD ( $\pm$ SD). The ratio for Q71-C homozygotes was not calculated but is expected to be a maximum of double the value shown for their heterozygous parents (Q71-C). Q71 transgenic mice developed the abnormal behavior described in the following figures and had premature death (age at death) or had a normal behavior and were killed at 15 months of age ( $>15$ ).

Using a cohort of 15 animals, we determined that Q71-B and Q71-C homozygotes died prematurely, whereas the heterozygous parents and Q20 transgenic mice, like wild-type mice, were alive until they were killed at 15 months of age (supplemental material, available at [www.jneurosci.org](http://www.jneurosci.org)).

### Pathology

#### Intranuclear inclusions

Neuronal intranuclear inclusions have been detected in brain regions severely and nonseverely affected in MJD (Paulson et al., 1997b; Schmidt et al., 1998; Yamada et al., 2001). We searched for neuronal intranuclear inclusions in brain and spinal cord sections of transgenic mice stained with ataxin-3 antibody 146 or 144 (Fig. 4). We note that a few subpopulations of neurons throughout the brain and spinal cord of all our transgenic mice had variable ataxin-3 immunostaining intensity and subcellular distribution (data not shown).

Q20-A transgenic and wild-type mouse neurons of midline deep cerebellar nuclei had no intranuclear inclusions, and ataxin-3 immunostaining was enriched in the cytoplasm (Fig. 4A). Similar results were observed in neurons of the olfactory bulb, cerebral cortex, hippocampus, thalamus, cerebellar cortex, dentate nuclei, pons, medulla, or spinal cord (data not shown).

In neurons of Q71-B homozygotes and Q71-E transgenic mice (Fig. 4A,B), Q71-C homozygotes (Fig. 4D), and Q71-I founder (data not shown), the ataxin-3 immunostaining was enriched in the nucleus and in intranuclear inclusions. The inclusions were more prominent (much larger and more abundant) in selective brain regions and spinal cord (Table 1). In spinal cord, the inclusions were detected in motor neurons (Fig. 4B) and sensory neurons (data not shown).

In neurons of Q71-B heterozygotes, intranuclear inclusions the size of the nucleolus were absent, although the ataxin-3 immunostaining was enriched in the nucleus (Fig. 4B). Similar results were observed in Q71-A heterozygotes (data not shown). In

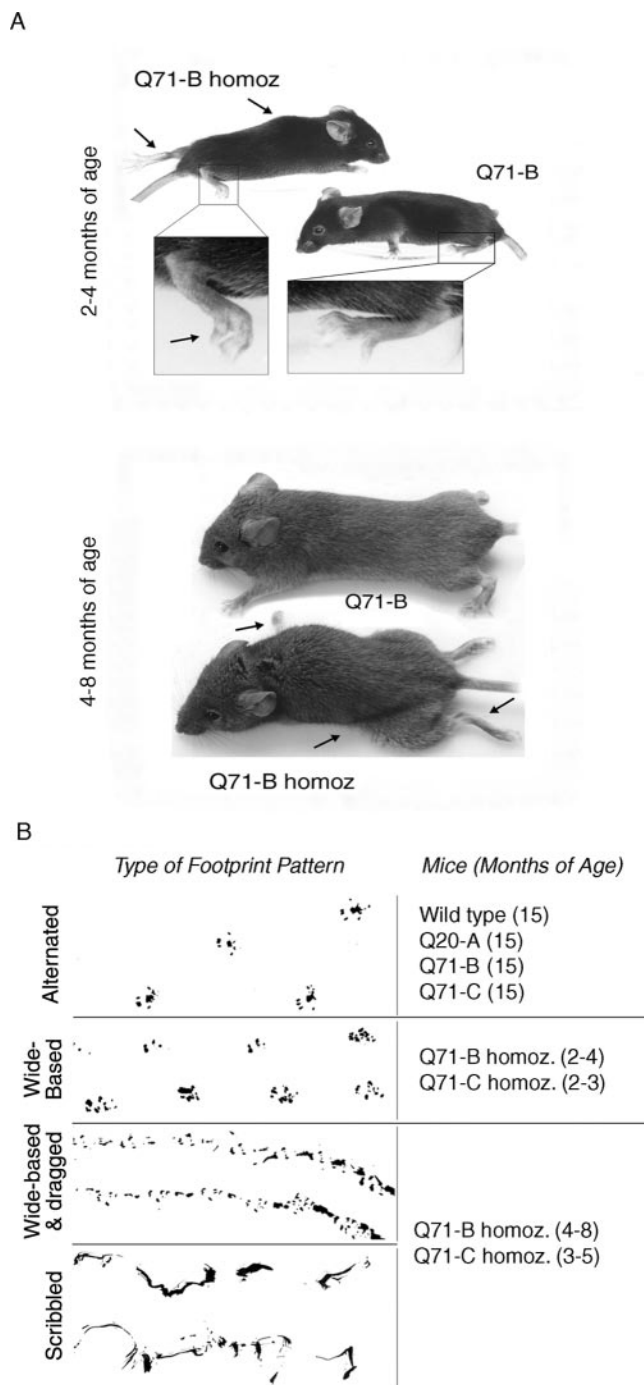


**Figure 2.** Appearance and gait of Q71 and Q20 transgenic mice. *A*, Q71-B homozygotes (Q71-B homozygote) 2–4 months of age had a small hunchback, transiently clutched paws, and uncoordinated extension of hindlimbs (arrows). At 4–8 months of age, they had pronounced hunchback with low pelvic elevation and muscle wasting, permanently clutched paws, and uncoordinated movement of extended limbs (arrows). Q71-B heterozygotes (Q71-B) of the same age and sex had the appearance and behavior of wild-type mice. *B*, The indicated Q71 transgenic mice at the specified ages developed a progressive deteriorating footprint pattern (wide-based at an early stage, wide-based and dragged at a late stage, and scribbled at a later to moribund stage). The remainder of the transgenic mice listed, like wild-type mice, had a normal alternative footprint pattern.

contrast, 13-month-old Q71-C heterozygotes had intranuclear inclusions the size of the nucleolus in neurons of deep cerebellar nuclei (Fig. 4C), pontine nuclei, and in spinal cord, but not in the rest of the brain regions analyzed (data not shown).

### Neurodegeneration

Neuronal loss in MJD occurs in selective brain regions such as dentate nuclei and substantia nigra (see Introduction). We searched for evidence of neurodegeneration in the transgenic mice. The brain sections of transgenic and wild-type mice stained for total proteins (eosin) and nucleic acids (hematoxylin), treated with transferase-mediated deoxyUTP nick end labeling, or immunostained for glial fibrillary acid protein had no qualitative morphological differences (data not shown).

Using unbiased stereology, we searched for differences in the number of neurons in dentate nuclei and dopaminergic (TH-positive) neurons in the substantia nigra. No significant differences were found in the total numbers of neurons in the dentate nucleus of the Q71-B and Q71-C homozygotes compared with Q20-A transgenic mice (Table 2).

The total number of TH-positive neurons in the substantia nigra of Q71-C homozygotes was 38% lower than in Q20-A transgenic mice (Table 2). By ANOVA, this 38% reduction in the Q71-C homozygotes was statistically significant ( $F_{(1,9)} = 6.34$ ;  $p < 0.04$ ). There was no significant reduction in the number of TH-positive neurons in Q71-B homozygotes compared with Q20-A transgenic mice ( $F_{(1,10)} = 3.35$ ;  $p < 0.10$ ). However, power analysis indicated that by analyzing two more Q71-B homozygotes and two more Q20-A transgenic mice the significant difference would be detected. The decrease in the number of TH-positive neurons in the substantia nigra of the Q71-C homozygotes compared with the Q71-B homozygotes paralleled the earlier age at death in the Q71-C homozygotes compared with Q71-B homozygotes.

In summary, Q71 transgenic mice with abnormal behavior had prominent neuronal intranuclear inclusions in selective brain regions and in spinal cord. The neuronal intranuclear inclusions the size of the nucleolus or larger were either not detected (Q71-B and Q71-A heterozygotes, Q20-A and Q20-B transgenic mice) or scarce (Q71-C heterozygotes) in animals with a normal behavior. Immunostaining for mutant ataxin-3 was enriched in the nucleus, and normal ataxin-3 in the cytoplasm of the neurons was analyzed. Decreased TH-positive cells in the substantia nigra were observed in Q71-C and possibly Q71-B homozygotes but not in Q20-A transgenic mice.

### Mutant ataxin-3 putative–cleavage fragment in brain of transgenic mice

A toxic cleavage fragment of mutant ataxin-3 md1a was proposed to trigger neurodegeneration (Ikeda et al., 1996). Such a fragment has not been detected in the brains of MJD patients (Paulson et al., 1997a; Berke et al., 2004) or transgenic mice (Cemal et al., 2002).

We detected readily the full-length form of mutant ataxin-3 by analyzing small amounts of Q71 transgenic mouse brain homogenates (Fig. 1, left blot). By analyzing larger brain samples and nuclear fractions and including the stacking gel during the transfer of proteins to nitrocellulose, we detected a mutant ataxin-3 putative–cleavage fragment (Fragment) and an aggregate (which appeared as a smear) (Fig. 5A, top blot). Full-length mutant ataxin-3 (58–64 kDa) was more nuclear in Q71-B homozygotes than in Q71-B heterozygotes. The fragment (36 kDa) was enriched in the nuclear fraction (Fig. 5A, top blot), abundant in sick Q71 transgenic mice, and scarce in healthy Q71 transgenic mice (Fig. 5A, bottom blot). The aggregate (>220 kDa) was enriched in the nuclear fraction and more abundant in sick Q71 transgenic mice (including Q71-B homozygotes) than in healthy animals (including Q71-B heterozygotes) (Fig. 5, top blot). Nor-

mal human (44 kDa) and mouse (43 kDa) ataxin-3 were enriched in the cytoplasmic fraction (Fig. 5, top blot). The enrichment of mutant ataxin-3 in the nuclear fraction and of normal ataxin-3 in the cytoplasmic fraction was consistent with the subcellular localization results described above (Fig. 4A).

The mutant ataxin-3 full-length form, but not fragment or aggregate, was detected in the gonads, muscle, or heart of transgenic mice (data not shown). Thus, the fragment and aggregate were brain specific. The abundance of the full-length form was similar in all brain regions and spinal cord (Fig. 5B; supplemental material, available at [www.jneurosci.org](http://www.jneurosci.org)). For example, the full-length mutant ataxin-3 in cerebellum over the cerebral cortex in Q71-B homozygotes was  $1 \pm 0.01$ . The fragment and aggregate were detected throughout the brain and in spinal cord but were more abundant in the cerebellum (Fig. 5B; supplemental material, available at [www.jneurosci.org](http://www.jneurosci.org)), which correlates with cerebellar nuclei having larger inclusions. The other brain regions with large inclusions, such as pontine nuclei, were homogenized with regions with small inclusions, such as medulla. Thus, it remains to be determined whether all brain regions with larger inclusions had more abundant aggregate and fragment.

We excluded the possibility that the cleavage fragment was an isoform resulting from alternative splicing by subjecting transgenic mouse brain mRNA to a reverse transcriptase (RT)-PCR (Fig. 5C). Only one PCR product was detected for each set of primers used; the PCR product in each reaction had the size expected on the basis of the ataxin-3 mjd1a sequence (Kawaguchi et al., 1994). RT-PCRs that included primers with nucleotides 13–904 and 1047–1713 also rendered a single product of the expected size (data not shown). We did not detect PCR products with the use of wild-type mouse brain mRNA because the nucleotide sequence of one of the primers used (antisense 1713) was human specific. The sequence is not conserved in murine ataxin-3 cDNA (National Center for Biotechnology Information nucleotide accession number NM029705). These results confirmed that the cleavage fragment was a product of a processing event at the protein level rather than the RNA level.

### Composition of the mutant ataxin-3 putative–cleavage fragment

Previous reports indicated that a C-terminal portion of mutant ataxin-3 mjd1a containing the polyglutamine expansion was cytotoxic, whereas the full-length form was not (Ikeda et al., 1996;

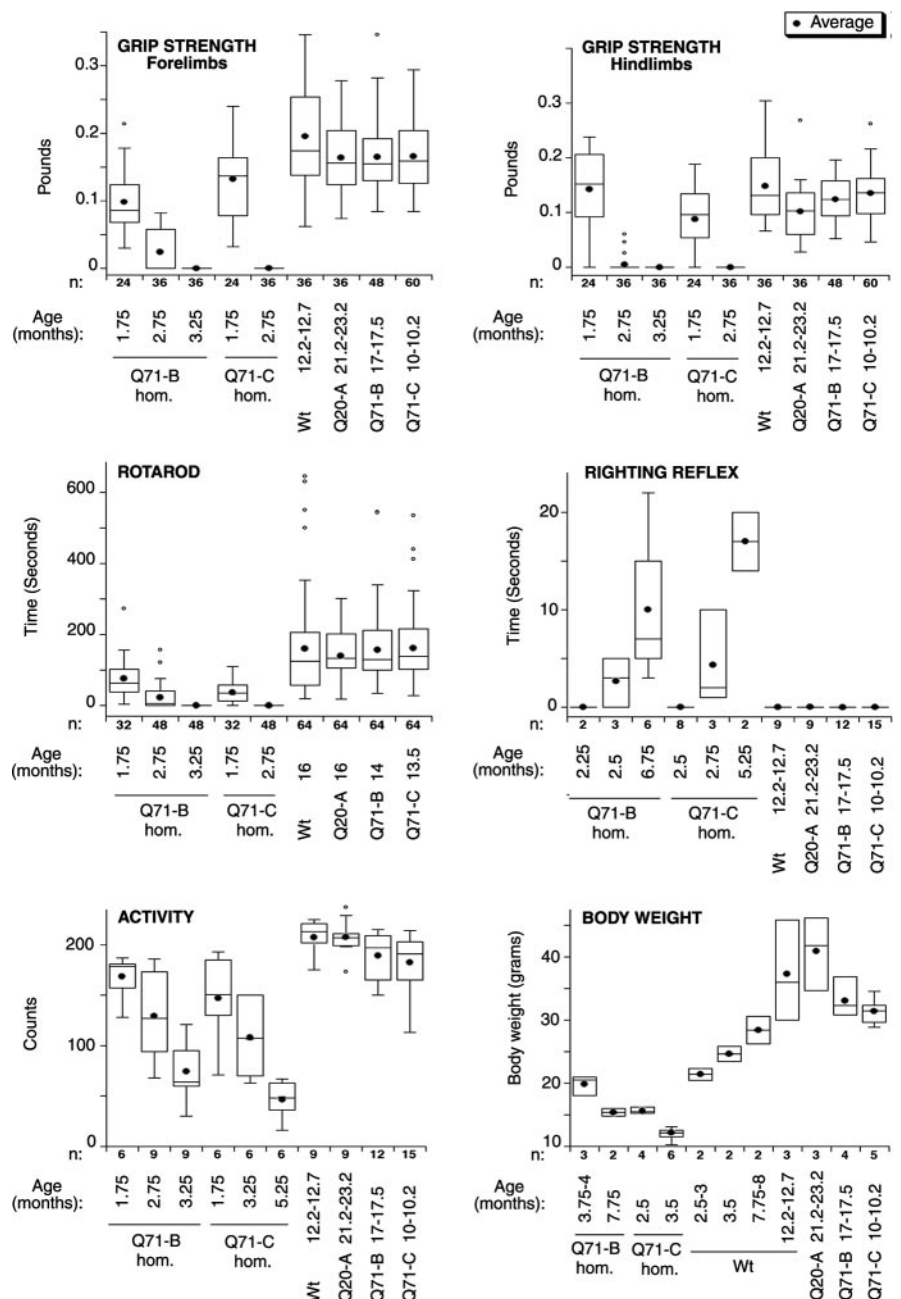


**Figure 3.** Behavioral test and body weight of Q71 and Q20 transgenic mice. For each animal indicated, we determined the following: grip strength, the force (in pounds) needed to release the grip of a rod; Rotarod, the time (in seconds) taken to fall off an accelerating rod; righting reflex, the time (in seconds) required for the mouse to turn its body to a normal position after being placed on its back; activity, the counts detected by a passive infrared activity monitor; and body weight. The values obtained for a given group of animals on different trials on consecutive days were pooled ( $n$  = total number of values) and are represented in a box plot. The black circle represents the average, and the line dividing the box represents the median; one-fourth of the data fall between the bottom of the box and the median, and another one-fourth fall between the median and the top of the box. The lines attached to the box extend to the smallest and the largest data values. Outliers are indicated as small circles and defined as values smaller than the lower quartile minus 1.5 times the interquartile range or larger than the upper quartile plus 1.5 times the interquartile range. hom., Homozygotes; Wt, wild type.

Paulson et al., 1997b; Warrick et al., 1998; Yoshizawa et al., 2000). Thus, we determined whether the putative–cleavage fragment that we detected in brain corresponded to a C-terminal portion of mutant ataxin-3 mjd1a containing the polyglutamine expansion. For this purpose, we used a panel of different ataxin-3-specific antibodies, antibody 1C2, and brain homogenate of Q71-H founder (Fig. 6A). All of the ataxin-3 antibodies recognized the

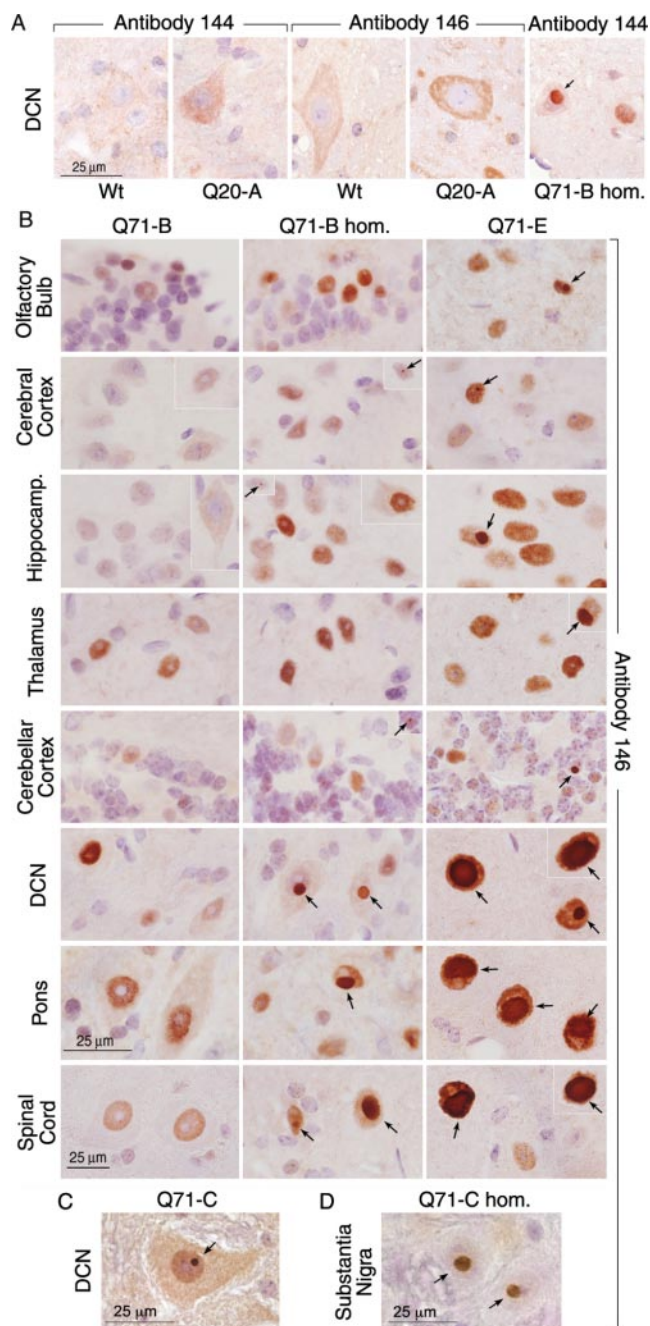


**Figure 4.** Ataxin-3-immunostained neurons from Q71 and Q20 transgenic mice. Paraffin-embedded midsagittal brain and spinal cord sections of the indicated animals were stained with ataxin-3 antibody 146 or 144, as indicated, counterstained with hematoxylin, and analyzed by light microscopy. An inset of an additional image of a neuron is included where necessary, to provide a better representation of the data. The magnification of brain images is the same for all samples and is represented with a bar. The magnification in all spinal cord images is slightly higher and represented by a different length bar. The intranuclear inclusions are highlighted (arrows). *A*, Images of deep cerebellar nuclei (DCN) neurons of wild-type mice (Wt; 12 months of age), Q20-A transgenic mice (6 months of age), and Q71-B homozygotes (Q71-B hom.; 4 months of age). *B*, Images of neurons from the indicated brain regions of a 4-month-old Q71-B heterozygote (Q71-B) and Q71-B homozygote (Q71-B hom.) and a 2.2-month-old Q71-E transgenic mouse. *C*, Image of a deep cerebellar nuclei (DCN) neuron from a Q71-C heterozygote at 13 months of age. *D*, Image of substantia nigra neurons of a 2.2-month-old Q71-C homozygote (Q71-C hom.) at 2.75 months of age.

doublet of mutant ataxin-3 full-length form. All antibodies reacted with the mutant ataxin-3 aggregate, except for 1C2, probably because of a conformational change as reported for other polyglutamine proteins (Poirier et al., 2002). Antibodies 1H9,

**Table 1. Quantitation of neuronal intranuclear inclusions the size of the nucleolus or larger in brain and spinal cord of Q71-B homozygotes**

Brain region (midline sections) or spinal cord (few sections)	Percentage of neurons with intranuclear inclusions the size of the nucleolus or larger ( $\pm$ SD)	
	Q71-B hom (3–4 months of age)	Q71-B hom (8 months of age)
Olfactory bulb	6 $\pm$ 4	23 $\pm$ 10.5
Frontal cortex	0	0
Hippocampus	0	0
Thalamus	0	1.5 $\pm$ 2.5
Cerebellum cortex	0	1 $\pm$ 2.5
Deep cerebellar nuclei	18 $\pm$ 6.5	41 $\pm$ 11
Pontine nuclei	15 $\pm$ 11	41 $\pm$ 6.5
Spinal cord	16.5 $\pm$ 7.5	21.5 $\pm$ 12.5

Paraffin-embedded spinal cord and midsagittal brain sections of 3- to 4-month-old and 8-month-old Q71-B homozygotes (hom) were stained with ataxin-3 antibody 146, counterstained with hematoxylin, and analyzed by light microscopy. We determined the percentage of neurons with intranuclear inclusions the size of the nucleolus or larger in each microscopic field (20 neurons per field). The results are the average of the values obtained in three to six fields (60–120 neurons per brain region or spinal cord) with the corresponding SD.

**Table 2. Quantitation of Nissl-stained neurons in dentate nuclei (DN) and TH-positive neurons in the substantia nigra (SN) using unbiased stereology**

Transgenic mice ( <i>n</i> )	Mean of total number neurons in DN ( $\pm$ SD)	Mean of total number TH-positive neurons in SN ( $\pm$ SD)
Q20-A (5)	1408 $\pm$ 630	1431 $\pm$ 640
Q71-B hom (5)	1625 $\pm$ 727	1158 $\pm$ 518
Q71-C hom (4)	1054 $\pm$ 527	894 $\pm$ 447 <sup>a</sup>

We used 6.5- to 7-month-old Q20-A and Q71-B homozygotes (hom) and 2- to 2.75-month-old Q71-C homozygotes. The results are the mean of the values obtained in four to five (*n*) of each of the indicated transgenic mice and the corresponding SD.

<sup>a</sup>The values of Q71-C homozygotes and Q20-A transgenic mice were significantly different (*t* test; *p* < 0.04).

1C2, and 146, but not 144 and 2B6, reacted with the fragment. Our antiserum to a peptide corresponding to amino acids 261–270 reacted with the aggregate, full-length form and fragment of mutant ataxin-3 (data not shown). Thus, the mutant ataxin-3 fragment contained the polyglutamine expansion, and the epitopes N terminal to residue 221 and C terminal to residue 334 were either hidden or missing.

Several caspase cleavage sites have been predicted for ataxin-3 (Wellington et al., 1998; Berke et al., 2004). To determine whether the mutant ataxin-3 fragment comigrated with predicted caspase cleavage products of the disease protein, we generated three plasmid DNA constructs encoding mutant (Q71) or normal (Q20) ataxin-3 mjd1a missing amino acids 1–145 ( $\Delta$ N145), 1–171 ( $\Delta$ N171), or 1–225 ( $\Delta$ N225). According to the literature on caspases (Stennicke and Salvesen, 1999), these constructs would be the predicted products of processing at sites 142-LISD-145, 168-DLPD-171, and 222-LDED-225, respectively. The constructs were expressed in a transfected neuroblastoma cell line, Neuro-2a. The truncated mutant ataxin-3 missing amino acids 1–225 (Q71 $\Delta$ N225) was the one most similar to the cleavage fragment (Fig. 6*B*). These data suggested that the fragment could be missing residues 1–225 if cleavage occurred at site 222-LDED-225.

The most important amino acid sequence of the 1H9 epitope was 221-MLDE-224 (Fig. 6*C*). 1H9 did not react with the construct missing residues 1–225 (Q71 $\Delta$ N225) but did react with constructs missing residues 1–145 (Q71 $\Delta$ N145) and 1–171 (Q71 $\Delta$ N171) (data not shown). Given that 1H9 bound to the mutant ataxin-3 fragment in brain, the residues 221–224 recognized by this antibody are included in the fragment. Therefore,

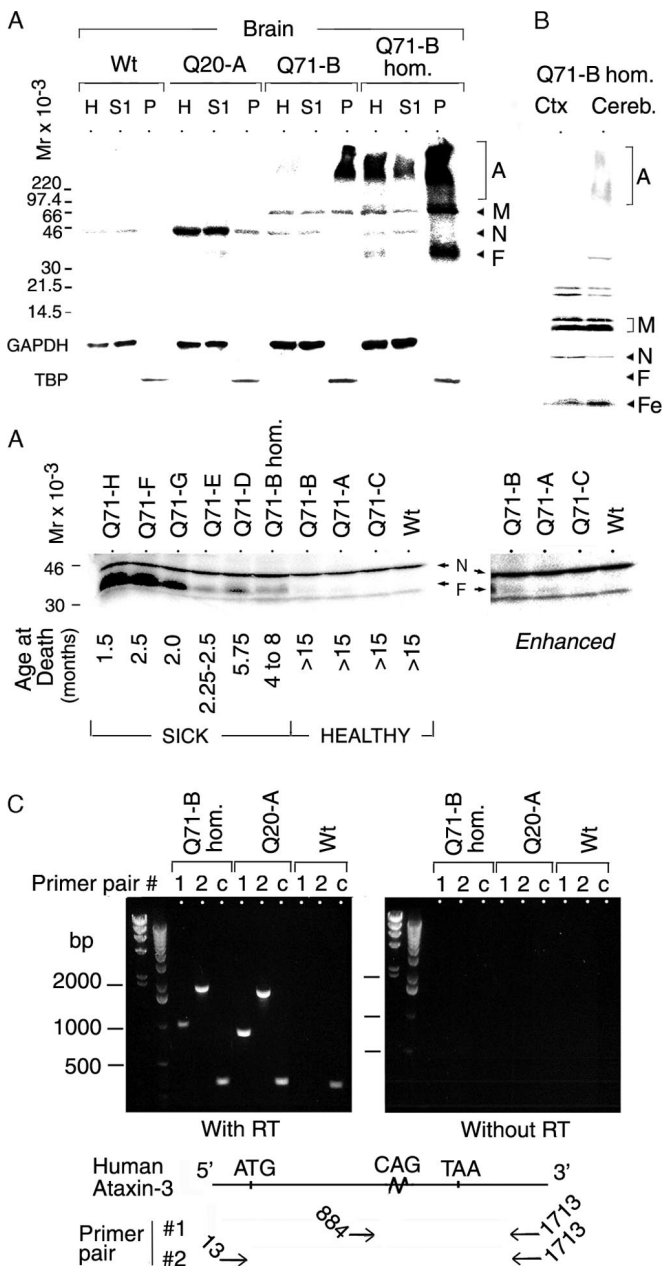


**Figure 5.** Mutant ataxin-3 putative cleavage fragment in brains of transgenic mice. *A*, Top and bottom, Western blot of brain homogenates (H) and cytoplasmic (S1) and purified nuclear (P) fractions from wild-type mice (Wt) and the indicated transgenic mice [all heterozygous, except for Q71-B homozygotes (Q71-B hom.)]. The blot was developed with antibody to full-length ataxin-3 (top blot), or as indicated to GAPDH (a cytoplasmic fraction marker) or TBP (a nuclear fraction marker). Bottom, Western blot of brain homogenates from the indicated Q71 transgenic mice and wild-type mice. The right portion of the blot is also shown as an enhanced image (Enhanced). The age at death of the “sick” Q71 transgenic mice is indicated. The “healthy” Q71 transgenic mice had no premature death (>15). Mutant ataxin-3 aggregate (A), full-length form (M), fragment (F), and normal human or murine ataxin-3 (N) are highlighted. *B*, Western blot of cerebral cortex (Ctx) or cerebellum (Cereb.) homogenates from 4-month-old Q71-B homozygotes (Q71-B hom.). The same amount of protein was analyzed per sample. The blot was developed using the antibody to full-length ataxin-3. Mutant ataxin-3 aggregate (A), full-length form (M), fragment (F), and murine ataxin-3 (N) are highlighted. An enhanced image of the portion of the blot that included the mutant ataxin-3 fragment is shown (Fe). *C*, RT-PCR of brain mRNA from the indicated transgenic and wild-type mice using the indicated pairs of primers. The pairs of primers #1 and #2 are represented under the diagram of the primary structure of human ataxin-3 mjd1a cDNA. The nucleotide number at the 5' end of each primer is indicated on an arrow. As a control (C), RT-PCR of the same mRNA brain samples was done using primers specific for 18S rRNA. We did the reaction with or without RT, as indicated. The size markers were Lambda DNA *Hind*III (first lane) and 1 kb ladder (second lane).

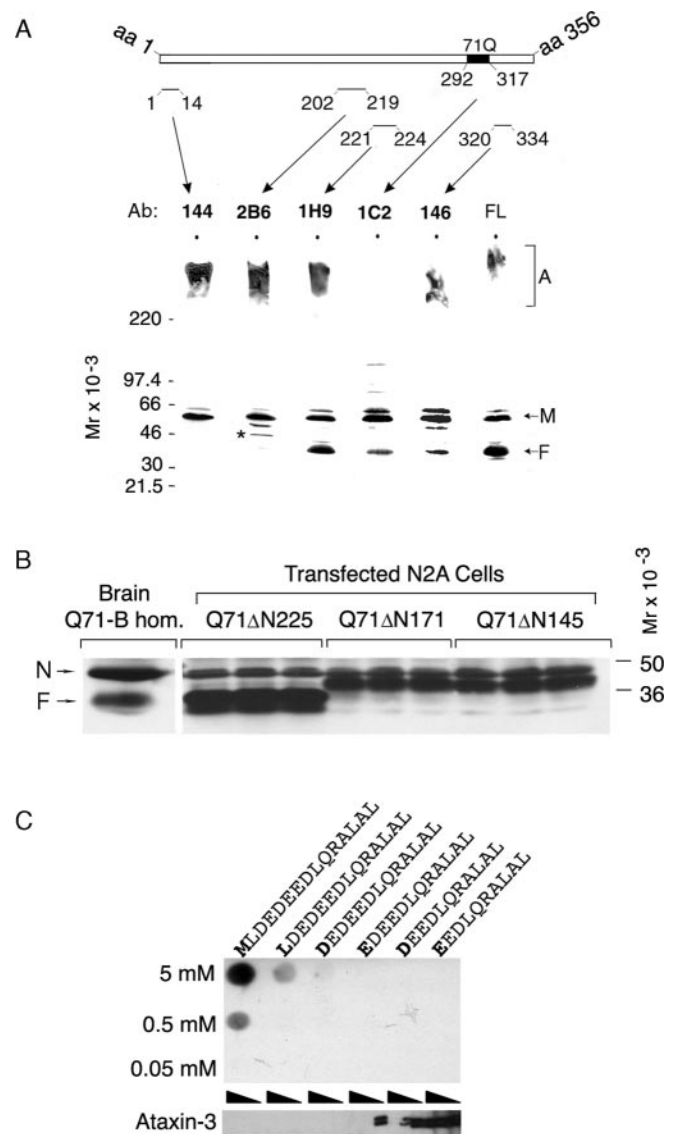


**Figure 6.** Composition of the mutant ataxin-3 putative cleavage fragment. *A*, Western blot of a brain homogenate of a Q71 transgenic mouse founder (Q71-H) with higher transgene expression levels than Q71-B homozygotes. The blot strips were developed with the ataxin-3 antibodies (Ab) indicated. Antibody 1C2 recognizes preferentially expanded polyglutamines. The antibody labeled here as FL was generated against full-length ataxin-3. The asterisk in the 2B6 blot highlights a nonspecific protein detected with the same intensity in the wild-type mouse brain. Mutant ataxin-3 aggregate (A), full-length form (M), and fragment (F) are highlighted. Normal murine ataxin-3 was detected in a longer exposure of the blot (data not shown). *B*, Western blot of lysates from transiently transfected Neuro-2a cells expressing human mutant ataxin-3 mjd1a with a 71 glutamine expansion and missing amino acid residues 1–225 (Q71ΔN225), 1–171 (Q71ΔN171), or 1–145 (Q71ΔN145). Q71-B homozygote brain homogenate (Q71-B hom.) was included as reference to determine which construct was similar in size to the mutant ataxin-3 cleavage fragment. The same amount of protein was analyzed per sample; the lysates were included in triplicate. The blots were developed using an antibody to full-length ataxin-3. Mutant ataxin-3 fragment (F) and normal murine ataxin-3 (N) are highlighted. We note that a higher molecular weight band was detected with all constructs (data not shown), which could be the result of oligomerization resistant to reducing conditions. *C*, Fine epitope mapping of 1H9 monoclonal antibody was performed using dot blot and competitive assays. Six synthetic polypeptides were designed with the first five amino acids of 221-MLDEEEDLQRALAL-235 antigenic polypeptide gradually removed. On the dot blot assay (top), increasing amounts of the polypeptides were dotted on nitrocellulose membrane and then immunodetected with 1H9 antibody. For the competitive assay (bottom), 1H9 antibody was preincubated with increasing amounts of the polypeptides (excess of 1, 100, or 1000 molar ratio) before incubation with the Western blot strips containing a protein extract from human lymphoblasts.

the brain mutant ataxin-3 fragment was not a product of cleavage at the caspase site 222-LDED-225 but could be a product of the predicted caspase site 214-EAND-217 (Berke et al., 2004).

### Cytotoxicity of truncated mutant ataxin-3

The mutant ataxin-3 fragment was abundant in the brains of our transgenic mice with an abnormal phenotype and was scarce in transgenic mice with a normal phenotype. A cell model was used to determine whether the fragment was neurotoxic above a critical concentration. Specifically, we used the truncated portion of mutant ataxin-3 mjd1a similar in composition to the fragment Q71ΔN225. Indeed, Q71ΔN225 but not Q71ΔN145 or Q71ΔN171 caused toxicity in a transfected neuroblastoma cell line (Fig. 7A). Neither human normal ataxin-3 mjd1a missing amino acid residues 1–225 (Q20ΔN225) nor full-length mutant ataxin-3 mjd1a were cytotoxic (Fig. 7A). Q71ΔN225 was less cytotoxic than HA-Q83, a construct generated previously that consists of a stretch of 83 glutamines tagged at the N terminus with a hemagglutinin (HA) epitope (Ikeda et al., 1996). Using an LDH-release assay, we confirmed the toxicity of constructs Q71ΔN225 and HA-Q83 but not pcDNA3 vector in transfected Neuro-2a cells. In a typical assay done in triplicate, the mean of the relative absorbance units (and SDs) were 0.57 ( $\pm 0.002$ ), 0.81 ( $\pm 0.143$ ), and 0.45 ( $\pm 0.22$ ), respectively. The differences between the constructs and the vector were significant (*t* test; *p* < 0.01). Using the luciferase assay, which was more sensitive than the LDH assay, we determined that the cytotoxicity of Q71ΔN225 and HA-Q83 occurred above a critical concentration in the transfected neuroblastoma cell line (Fig. 7B). The cytotoxicity results were consistent with the hypothesis that the mutant ataxin-3 cleavage fragment was toxic above a critical concentration.

### Mutant ataxin-3 putative–cleavage fragment in brain of MJD patients

To determine whether the fragment could be associated with neuronal loss in MJD patients, the brain regions affected (dentate nuclei and substantia nigra) and a brain region typically spared from severe neuronal loss (frontal cortex) were analyzed.

A mutant ataxin-3 fragment was enriched in the nuclear fractions of postmortem brain tissue from all of the MJD heterozygous patients that we analyzed: case numbers 2024, 1704 (Fig. 8A), and 1965 (data not shown). The fragment was ~30 kDa smaller than the full-length form, which corresponded to 35 kDa in patient 2024. It was more abundant in the substantia nigra (Fig. 8A) and cerebellum (dentate nuclei) (Fig. 8B) than in the cerebral cortex (Fig. 8A, B). A similar size band was not detected in the cerebellum (dentate nuclei) of two normal individuals, including number 48,108 (Fig. 8B); we note that we observed variations between samples depending on how they were processed. Thus, a putative–cleavage fragment of mutant ataxin-3 was generated in the MJD patient brain and more abundant in two severely affected brain regions.

In addition, the mutant and normal ataxin-3 full-length forms were enriched in the nuclear fraction in MJD patients (Fig. 8A). The sample from MJD patient 2024 had a scarce nuclear aggregate (>220 kDa) (Fig. 8A). The neuronal nuclear inclusions in MJD patients were immunostained with ataxin-3 antibodies 144 and 146 (Fig. 8C).

## Discussion

### MJD mouse model

Transgenic mice expressing truncated but not complete human mutant ataxin-3 isoform mjd1a under the control of the Purkinje

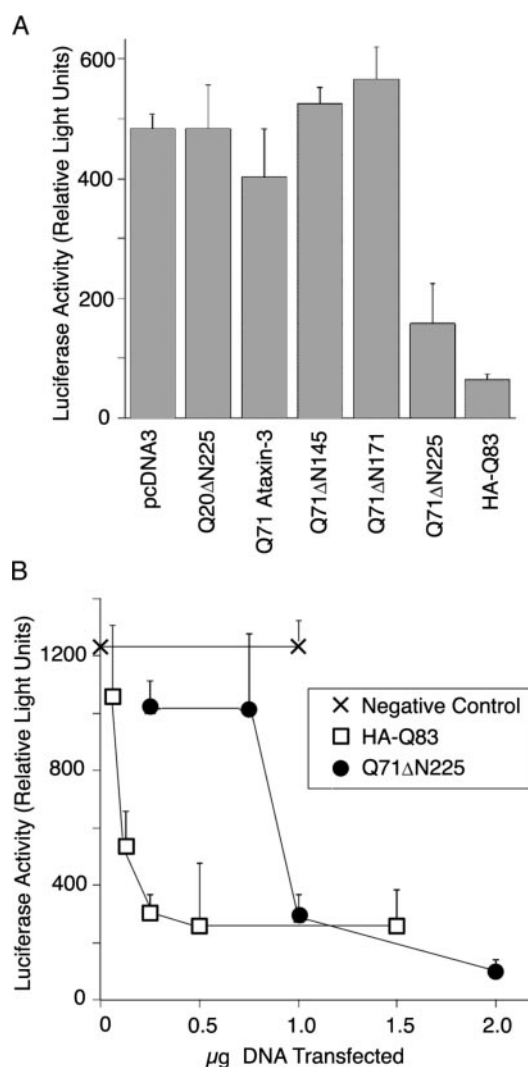


**Figure 7.** Cytotoxicity of truncated mutant ataxin-3. *A*, Luciferase activity in lysates of Neuro-2a cells transiently cotransfected with the pcDNA3 vector (pcDNA3) or the indicated pcDNA3 constructs and the pRL-SV40-Renilla luciferase plasmid. The constructs used were as follows: (1) human normal ataxin-3 mjd1a with a stretch of 20 glutamines and missing amino acid residues 1–225 (Q20ΔN225); (2) human mutant ataxin-3 mjd1a with a stretch of 71 glutamines (Q71-ataxin-3) or missing amino acid residues 1–145 (Q71ΔN145), 1–171 (Q71ΔN171), or 1–225 (Q71ΔN225); and (3) a stretch of 83 glutamines tagged at the N terminus with an HA epitope and previously generated (HA-Q83). The results are the mean of the values obtained in three experiments with the corresponding SD. *B*, Luciferase activity in lysates of Neuro-2a cells transiently transfected with 0.2  $\mu\text{g}$  of SV40-Renilla luciferase plasmid by itself (0  $\mu\text{g}$  of DNA transfected, negative control) or together with the indicated quantity of pcDNA3 vector (negative control), HA-Q83, or Q71ΔN225. The results are the mean of the values obtained in three experiments with the corresponding SD. For the 0.25  $\mu\text{g}$  of Q71ΔN225 point, the best two of three values were selected.

cell promoter developed an abnormal phenotype (Ikeda et al., 1996); however, Purkinje cells are poorly affected in MJD. We have now generated transgenic mice expressing the complete human mutant (Q71) or normal (Q20) ataxin-3 mjd1a under the control of the mouse prion promoter, to drive expression throughout the brain (Borchelt et al., 1996; Garden et al., 2002) and spinal cord. Q71 transgenic mice expressing mutant ataxin-3 above a critical level experienced a phenotype similar to MJD including progressive postural instability, gait and limb ataxia, weight loss, premature death, neuronal intranuclear inclusions, and decreased TH-positive neurons in the substantia nigra. Q20 transgenic mice had normal behavior and pathology.

The abnormal phenotype in our transgenic mice does not arise from generic toxicity caused by high transgene expression levels or gene alterations at the transgene integration site, based on the following rationale: (1) different Q71 founders and homozygotes had a similar abnormal phenotype; (2) transgenic mice expressing human normal ataxin-3 mjd1a at higher levels than mutant ataxin-3 mjd1a in our Q71 transgenic mice were normal; and (3) transgenic mice expressing other polyglutamine disease proteins under the control of the same mouse prion promoter had a different phenotype (Schilling et al., 1999; Garden et al., 2002). For instance, neuronal inclusions were readily detected in the cerebral cortex of the dentatorubropallidolusian atrophy (DRPLA) mouse model (Schilling et al., 1999), were absent in Purkinje cells of the SCA7 mouse model (Garden et al., 2002), and were barely detectable in our transgenic mice. Unlike our transgenic mice, by unbiased stereology, 9-month-old DRPLA transgenic mice (AT65Q line 150) had 30% fewer neurons in the dentate nuclei than age-matched controls (David Borchelt, personal communication).

An MJD mouse model was previously generated using a yeast artificial chromosome construct containing the MJD1 gene coding for alternative spliced isoforms of mutant ataxin-3 and flanking genes (Cemal et al., 2002). These transgenic mice developed mild motor deficit, no premature death, and, by qualitative analysis, a 40% neuronal loss in dentate nuclei, which has yet to be confirmed using quantitative methods. Our Q71 homozygotes expressing mutant ataxin-3 isoform mjd1a had a more severe motor deficit, premature death, and yet no neuronal loss in the dentate nucleus using rigorous stereological analysis. Thus, several alternative spliced isoforms of the disease protein might be contributing to MJD pathogenesis as proposed for SCA6 (Zhuchenko et al., 1997; Resituito et al., 2000).

The Q71 transgenic mice with slightly lower levels of transgene expression, such as the heterozygous parents of the sick Q71 homozygotes, had normal behavior until they were killed at 15 months of age and few or no large inclusions. These results are reminiscent of previously described transgenic mice expressing low levels of the disease polyglutamine protein for SCA1 that had mild or no pathology and normal behavior (Burrigh et al., 1995).

#### Mutant ataxin-3 putative–cleavage fragment

We have detected a mutant ataxin-3 mjd1a putative–cleavage fragment (37 kDa) in the brains of our Q71 transgenic mice. The fragment contained the polyglutamine expansion, was missing epitopes N terminal to residue 221, and nearly comigrated with truncated mutant ataxin-3 missing residues 1–225. Thus, the cleavage site is N terminal to amino acid residue 221. The protease(s) involved remain to be determined. It could be a caspase

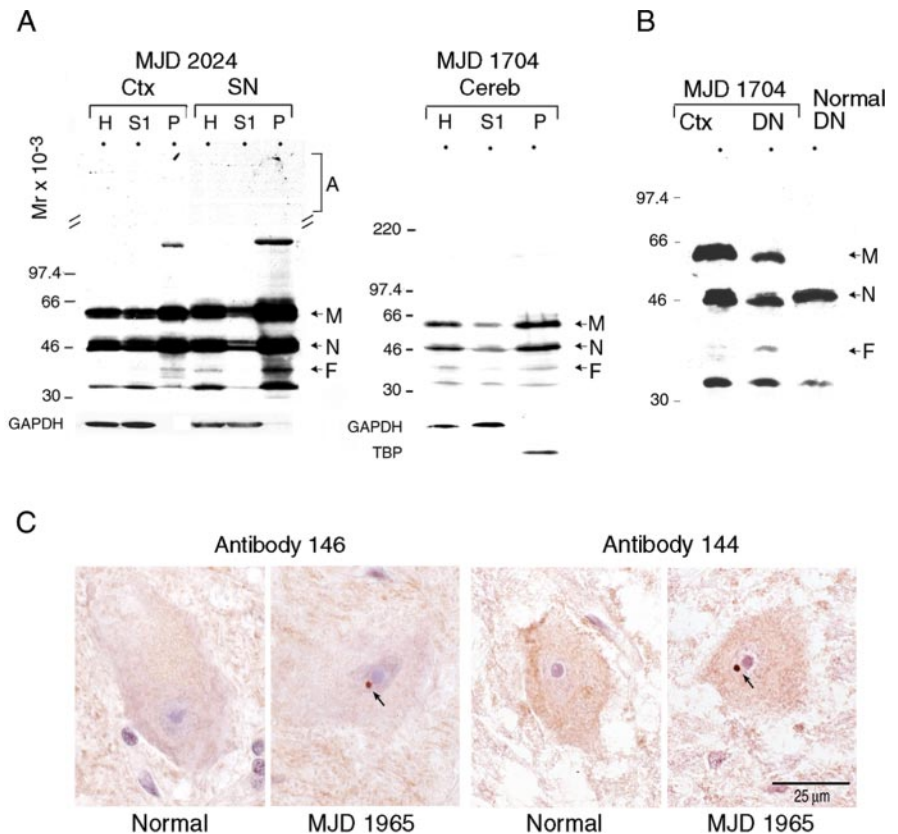


**Figure 8.** Mutant ataxin-3 cleavage fragment in the brain of an MJD patient. *A*, Western blots of homogenates (H) and cytoplasmic (S1) and purified nuclear (P) fractions from frontal cerebral cortex (Ctx), substantia nigra (SN), or cerebellar cortex/dentate nuclei (Cereb) from the indicated MJD heterozygous patients. The same amount of total protein was analyzed per sample, except for SN (1.5 times as much protein was used). The blots were developed using an antibody to full-length ataxin-3 (top blot) or, as indicated, GAPDH (a cytoplasmic fraction marker) or TBP (a nuclear fraction marker). The relative migration ( $M_r$ ) of each molecular weight standard used is indicated. Mutant ataxin-3 aggregate (A), full-length form (M), fragment (F), and normal ataxin-3 (N) are highlighted. *B*, Western blot of homogenates from frontal cerebral cortex (Ctx) or dentate nuclei (DN) of MJD heterozygous patient 1704 or normal DN from individual 48,108. The same amount of protein was analyzed per sample. The blot was developed using the full-length ataxin-3 antibody. *C*, Images of dentate nuclei neurons of the cerebellum from a normal individual or MJD heterozygous patient 1965. Paraffin-embedded sections were stained with ataxin-3 antibody 146 or 144, as indicated, counterstained with hematoxylin, and analyzed by light microscopy. The same magnification was used for all images and is represented with a bar.

cleaving at 214–EAND-217 (Berke et al., 2004) or, as reported for the cleavage fragment of other polyglutamine disease proteins, calpain or aspartic endopeptidases acting in concert with the proteasome (Kim et al., 2001; Gafni and Ellerby, 2002; Lunken et al., 2002; Sun et al., 2002; Gafni et al., 2004). We expect that the mutant ataxin-3 fragment in our transgenic mouse brain will serve as a reference to identify a cell model and cellular components relevant to the appropriate processing of the disease protein.

The mutant ataxin-3 putative–cleavage fragment in the brains of MJD patients could be a product of isoforms mjd1a and/or ataxin-3c (Kawaguchi et al., 1994; Schmidt et al., 1998; Ichikawa et al., 2001). We anticipate that the mechanism(s) of proteolytic processing will be the same for both isoforms because they share the sequence N terminal to the polyglutamine expansion.

The mutant ataxin-3 putative–cleavage fragment was abundant in the sick Q71 transgenic mouse brain and scarce in the healthy Q71 transgenic mouse brain. The fragment was more abundant in two MJD patient brain regions affected than in a spared one. The toxicity of truncated mutant ataxin-3 in transfected Neuro-2a cells required a critical concentration. Together,

these results indicate that MJD pathogenesis is associated with a critical concentration of the mutant ataxin-3 mjd1a fragment.

Mutant ataxin-3 expression throughout the brains of MJD patients is similar (Trottier et al., 1995, 1998; Nishiyama et al., 1996; Paulson et al., 1997a; Schmitt et al., 1997; Wang et al., 1997). Thus, the increased concentration of the mutant ataxin-3 putative–cleavage fragment in selective brain regions is unlikely to result from a higher level of mutant ataxin-3 expression. Variations in other cellular components such as proteolytic enzymes could be involved.

Our results are consistent with reports on other polyglutamine disorders. A cleavage fragment has been identified for several polyglutamine proteins, and in some reports its abundance is associated with pathogenesis (DiFiglia et al., 1997; Butler et al., 1998; Merry et al., 1998; Ellerby et al. 1999; Ona et al., 1999; Li et al., 2000; Mende-Mueller et al., 2001; Wellington et al., 2002). In a mouse model for DRPLA, the progressive severity of the disease was associated with increased abundance of a cleavage fragment (Schilling et al., 1999). In Huntington's disease, the cleavage fragment and the full-length disease protein were more abundant in affected than in spared regions of the patient's brain (Kim et al., 2001), which suggested that the increased abundance of the fragment could be attributable to a higher expression level. However, it remains to be determined whether the cleavage fragment in these other polyglutamine diseases is associated with cytotoxicity above a narrow critical concentration.

#### Nuclear localization of mutant ataxin-3 and model of MJD pathogenesis

By subcellular fractionation of brain and immunohistochemistry of neurons from our transgenic mice, mutant ataxin-3 was enriched in the nucleus and normal ataxin-3 was mostly cytoplasmic. Similar data were obtained by ataxin-3 immunostaining neurons of previously reported transgenic mice (Cemal et al., 2002). These results are not consistent with the data we obtained (Fig. 8) and were reported using human tissue (Paulson et al., 1997a; Fujigasaki et al., 2000), which could be attributable to autolysis caused by postmortem delay. In a cell line, normal ataxin-3 was reported to be nuclear (Tait et al., 1998), but cell lines can lose genetic material. Thus, based on the transgenic mouse data, we conclude that the polyglutamine expansion causes the nuclear localization of human mutant ataxin-3 mjd1a in neurons.

Intranuclear inclusions in transgenic mouse and MJD patient neurons were revealed with ataxin-3 antibodies to epitopes N or C terminal to the polyglutamine region. This is not consistent with antibody 2B6 recognizing an epitope N terminal to the polyglutamine region but not reacting with neuronal inclusions in MJD patients (Paulson et al., 1997b; Schmidt et al., 1998). Because 2B6 revealed the mutant ataxin-3 aggregate (Fig. 6A), the epitope 2B6 recognizes could be hidden in intranuclear inclusions. We observed that mouse ataxin-3 appeared to remain in the cytoplasmic fraction of the Q71 transgenic mouse brain (Fig. 5A). Thus, we suggest that full-length human mutant but not murine ataxin-3 is localized in the inclusions in Q71 transgenic mice.

The same immunostaining pattern of neurons with ataxin-3 antibodies to epitopes N or C terminal to the polyglutamine region suggests that the mutant ataxin-3 fragment either colocalizes with the full-length form or is not generated in neurons. Truncated mutant ataxin-3 aggregates and recruits the full-length disease protein in transfected cells (Paulson et al., 1997b; Perez et al., 1998). Therefore, the mutant ataxin-3 fragment is

likely to be generated in neurons and colocalize with the full-length form by recruiting it into an aggregate or inclusion.

Three lines of Q71 heterozygotes had normal behavior, nuclear and scarce mutant ataxin-3 fragment and aggregate, and few or no large intranuclear inclusions. Thus, nuclear localization and the formation of fragment and aggregate/inclusions precede the abnormal behavior. We propose that the mutant ataxin-3 fragment above a critical concentration initiates pathogenesis. The aggregation of the fragment and the full-length form could be an attempt by neurons to stabilize the disease-causing protein, which in turn could contribute to many neuropathological phenotypes, such as the proposed exhaustion of the components of proteasome protein degradation (Sherman and Goldberg, 2001).

In summary, a mouse model for mutant ataxin-3 mjd1a toxicity is proposed and characterized. One use for this model will be the development of strategies for the therapeutic management of pathogenesis caused by mutant ataxin-3 mjd1a. Based on the findings presented, decreasing mutant ataxin-3 mjd1a expression or the concentration of its putative–cleavage fragment below a critical level could be explored as a goal for therapy.

#### References

- Berke SJ, Schmiegel FA, Brunt ER, Ellerby LM, Paulson HL (2004) Caspase-mediated proteolysis of the polyglutamine disease protein ataxin-3. *J Neurochem* 89:908–918.
- Blobel G, Potter VR (1966) Nuclei from rat liver: isolation method that combines purity with high yield. *Science* 154:1662–1665.
- Borchelt DR, Davis J, Fischer M, Lee MK, Slunt HH, Ratovitsky T, Regard J, Copeland NG, Jenkins NA, Sisodia SS, Price DL (1996) A vector for expressing foreign genes in the brains and hearts of transgenic mice. *Genet Anal* 13:159–163.
- Burright EN, Clark HB, Servadio A, Matilla T, Feddersen RM, Yunis WS, Duvick LA, Zoghbi HY, Orr HT (1995) SCA1 transgenic mice: a model for neurodegeneration caused by an expanded CAG trinucleotide repeat. *Cell* 82:937–948.
- Butler R, Leigh PN, McPhaul MJ, Gallo JM (1998) Truncated forms of the androgen receptor are associated with polyglutamine expansion in X-linked spinal and bulbar muscular atrophy. *Hum Mol Genet* 7:121–127.
- Cemal CK, Carroll CJ, Lawrence L, Lowrie MB, Ruddle P, Al-Mahdawi S, King RH, Pook MA, Huxley C, Chamberlain S (2002) YAC transgenic mice carrying pathological alleles of the MJD1 locus exhibit a mild and slowly progressive cerebellar deficit. *Hum Mol Genet* 11:1075–1094.
- Clark HB, Burright EN, Yunis WS, Larson S, Wilcox C, Hartman B, Matilla A, Zoghbi HY, Orr HT (1997) Purkinje cell expression of a mutant allele of SCA1 in transgenic mice leads to disparate effects on motor behaviors, followed by a progressive cerebellar dysfunction and histological alterations. *J Neurosci* 17:7385–7395.
- DiFiglia M, Sapp E, Chase KO, Davies SW, Bates GP, Vonsattel JP, Aronin N (1997) Aggregation of huntingtin in neuronal intranuclear inclusions and dystrophic neurites in brain. *Science* 277:1990–1993.
- Durr A, Stevanin G, Cancel G, Duyckaerts C, Abbas N, Didierjean O, Chneiweiss H, Benomar A, Lyon-Caen O, Julien J, Serdaru M, Penet C, Agid Y, Brice A (1996) Spinocerebellar ataxia 3 and Machado-Joseph disease: clinical, molecular, and neuropathological features. *Ann Neurol* 39:490–499.
- Ellerby LM, Andrusiak RL, Wellington CL, Hackam AS, Propp SS, Wood JD, Sharp AH, Margolis RL, Ross CA, Salvesen GS, Hayden MR, Bredesen DE (1999) Cleavage of atrophin-1 at caspase site aspartic acid 109 modulates cytotoxicity. *J Biol Chem* 274:8730–8736.
- Fowler HL (1984) Machado-Joseph-Azorean disease. A ten-year study. *Arch Neurol* 41:921–925.
- Fujigasaki H, Uchiyama T, Koyano S, Iwabuchi K, Yagishita S, Makifuchi T, Nakamura A, Ishida K, Toru S, Hirai S, Ishikawa K, Tanabe T, Mizusawa H (2000) Ataxin-3 is translocated into the nucleus for the formation of intranuclear inclusions in normal and Machado-Joseph disease brains. *Exp Neurol* 165:248–256.

- Gafni J, Ellerby LM (2002) Calpain activation in Huntington's disease. *J Neurosci* 22:4842–4849.
- Gafni J, Hermel E, Young JE, Wellington CL, Hayden MR, Ellerby LM (2004) Inhibition of calpain cleavage of Huntingtin reduces toxicity: accumulation of calpain/caspase fragments in the nucleus. *J Biol Chem* 279:20211–20220.
- Garden GA, Libby RT, Fu YH, Kinoshita Y, Huang J, Possin DE, Smith AC, Martinez RA, Fine GC, Grote SK, Ware CB, Einum DD, Morrison RS, Ptacek LJ, Sopher BL, La Spada AR (2002) Polyglutamine-expanded ataxin-7 promotes non-cell-autonomous purkinje cell degeneration and displays proteolytic cleavage in ataxic transgenic mice. *J Neurosci* 22:4897–4905.
- Goldberg YP, Nicholson DW, Rasper DM, Kalchman MA, Koide HB, Graham RK, Bromm M, Kazemi-Esfarjani P, Thornberry NA, Vaillancourt JP, Hayden MR (1996) Cleavage of huntingtin by apopain, a proapoptotic cysteine protease, is modulated by the polyglutamine tract. *Nat Genet* 13:442–449.
- Greenfield JG, Lantos PL, Graham DI (2002) Greenfield's neuropathology, Ed 7. London: Arnold.
- Hara J, Beuckmann CT, Nambu T, Willie JT, Chemelli RM, Sinton CM, Sugiyama F, Yagami K, Goto K, Yanagisawa M, Sakurai T (2001) Genetic ablation of orexin neurons in mice results in narcolepsy, hypophagia, and obesity. *Neuron* 30:345–354.
- Harlow E, Lane D (1988) *Antibodies: a laboratory manual*, pp 82–83 Cold Spring Harbor, NY: Cold Spring Harbor Laboratory.
- Ichikawa Y, Goto J, Hattori M, Toyoda A, Ishii K, Jeong SY, Hashida H, Masuda N, Ogata K, Kasai F, Hirai M, Maciel P, Rouleau GA, Sakaki Y, Kanazawa I (2001) The genomic structure and expression of MJD, the Machado-Joseph disease gene. *J Hum Genet* 46:413–422.
- Ikeda H, Yamaguchi M, Sugai S, Aze Y, Narumiya S, Kakizuka A (1996) Expanded polyglutamine in the Machado-Joseph disease protein induces cell death in vitro and in vivo. *Nat Genet* 13:196–202.
- Israel M, Whittaker VP (1965) The isolation of mossy fibre endings from the granular layer of the cerebellar cortex. *Experientia* 21:325–326.
- Jardim LB, Silveira I, Pereira ML, Ferro A, Alonso I, do Ceu Moreira M, Mendonca P, Ferreirinha F, Sequeiros J, Giugliani R (2001) A survey of spinocerebellar ataxia in South Brazil—66 new cases with Machado-Joseph disease, SCA7, SCA8, or unidentified disease-causing mutations. *J Neurol* 248:870–876.
- Kawaguchi Y, Okamoto T, Taniwaki M, Aizawa M, Inoue M, Katayama S, Kawakami H, Nakamura S, Nishimura M, Akiguchi I (1994) CAG expansions in a novel gene for Machado-Joseph disease at chromosome 14q32.1. *Nat Genet* 8:221–228.
- Kim YJ, Yi Y, Sapp E, Wang Y, Cuiffo B, Kegel KB, Qin ZH, Aronin N, DiFiglia M (2001) Caspase 3-cleaved N-terminal fragments of wild-type and mutant huntingtin are present in normal and Huntington's disease brains, associate with membranes, and undergo calpain-dependent proteolysis. *Proc Natl Acad Sci USA* 98:12784–12789.
- Li H, Li SH, Johnston H, Shelbourne PF, Li XJ (2000) Amino-terminal fragments of mutant huntingtin show selective accumulation in striatal neurons and synaptic toxicity. *Nat Genet* 25:385–389.
- Lunkes A, Lindenberg KS, Ben-Haiem L, Weber C, Devys D, Landwehrmeyer GB, Mandel JL, Trotter Y (2002) Proteases acting on mutant huntingtin generate cleaved products that differentially build up cytoplasmic and nuclear inclusions. *Mol Cell* 10:259–269.
- Matilla T, McCall A, Subramony SH, Zoghbi HY (1995) Molecular and clinical correlations in spinocerebellar ataxia type 3 and Machado-Joseph disease. *Ann Neurol* 38:68–72.
- Mende-Mueller LM, Toneff T, Hwang SR, Chesselet MF, Hook VY (2001) Tissue-specific proteolysis of Huntingtin (htt) in human brain: evidence of enhanced levels of N- and C-terminal htt fragments in Huntington's disease striatum. *J Neurosci* 21:1830–1837.
- Merry DE, Kobayashi Y, Bailey CK, Taye AA, Fischbeck KH (1998) Cleavage, aggregation and toxicity of the expanded androgen receptor in spinal and bulbar muscular atrophy. *Hum Mol Genet* 7:693–701.
- Mouton PR, Gokhale AM, Ward NL, West MJ (2002) Stereological length estimation using spherical probes. *J Microsc* 206:54–64.
- Nishiyama K, Murayama S, Goto J, Watanabe M, Hashida H, Katayama S, Nomura Y, Nakamura S, Kanazawa I (1996) Regional and cellular expression of the Machado-Joseph disease gene in brains of normal and affected individuals. *Ann Neurol* 40:776–781.
- Ona VO, Li M, Vonsattel JP, Andrews LJ, Khan SQ, Chung WM, Frey AS, Menon AS, Li XJ, Stieg PE, Yuan J, Penney JB, Young AB, Cha JH, Friedlander RM (1999) Inhibition of caspase-1 slows disease progression in a mouse model of Huntington's disease. *Nature* 399:263–267.
- Orr HT (2001) Beyond the Qs in the polyglutamine diseases. *Genes Dev* 15:925–932.
- Paulson HL, Das SS, Crino PB, Perez MK, Patel SC, Gotsdiner D, Fischbeck KH, Pittman RN (1997a) Machado-Joseph disease gene product is a cytoplasmic protein widely expressed in brain. *Ann Neurol* 41:453–462.
- Paulson HL, Perez MK, Trotter Y, Trojanowski JQ, Subramony SH, Das SS, Vig P, Mandel JL, Fischbeck KH, Pittman RN (1997b) Intracellular inclusions of expanded polyglutamine protein in spinocerebellar ataxia type 3. *Neuron* 19:333–344.
- Paxinos G, Franklin KBJ (2001) *The mouse brain in stereotaxic coordinates*, Ed 2. London: Academic.
- Perez MK, Paulson HL, Pendse SJ, Saionz SJ, Bonini NM, Pittman RN (1998) Recruitment and the role of nuclear localization in polyglutamine-mediated aggregation. *J Cell Biol* 143:1457–1470.
- Poirier MA, Li H, Macosko J, Cai S, Amzel M, Ross CA (2002) Huntingtin spheroids and protofibrils as precursors in polyglutamine fibrilization. *J Biol Chem* 277:41032–41037.
- Restituto S, Thompson RM, Eliet J, Raike RS, Riedl M, Charnet P, Gomez CM (2000) The polyglutamine expansion in spinocerebellar ataxia type 6 causes a  $\beta$  subunit-specific enhanced activation of P/Q-type calcium channels in *Xenopus* oocytes. *J Neurosci* 20:6394–6403.
- Schilling G, Wood JD, Duan K, Slunt HH, Gonzales V, Yamada M, Cooper JK, Margolis RL, Jenkins NA, Copeland NG, Takahashi H, Tsuji S, Price DL, Borchelt DR, Ross CA (1999) Nuclear accumulation of truncated atrophin-1 fragments in a transgenic mouse model of DRPLA. *Neuron* 24:275–286.
- Schmidt T, Landwehrmeyer GB, Schmitt I, Trotter Y, Auburger G, Laccone F, Klockgether T, Volpel M, Epplen JT, Schols L, Riess O (1998) An isoform of ataxin-3 accumulates in the nucleus of neuronal cells in affected brain regions of SCA3 patients. *Brain Pathol* 8:669–679.
- Schmitt I, Brattig T, Gossen M, Riess O (1997) Characterization of the rat spinocerebellar ataxia type 3 gene. *Neurogenetics* 1:103–112.
- Schols L, Amoiridis G, Langkafel M, Buttner T, Przuntek H, Riess O, Vieira-Saecker AM, Epplen JT (1995) Machado-Joseph disease mutations as the genetic basis of most spinocerebellar ataxias in Germany. *J Neurol Neurosurg Psychiatry* 59:449–450.
- Sharp AH, Loev SJ, Schilling G, Li SH, Li XJ, Bao J, Wagster MV, Kotzok JA, Steiner JP, Lo A (1995) Widespread expression of Huntington's disease gene (IT15) protein product. *Neuron* 14:1065–1074.
- Sherman MY, Goldberg AL (2001) Cellular defenses against unfolded proteins: a cell biologist thinks about neurodegenerative diseases. *Neuron* 29:15–32.
- Silveira I, Coutinho P, Maciel P, Gaspar C, Hayes S, Dias A, Guimaraes J, Loureiro L, Sequeiros J, Rouleau GA (1998) Analysis of SCA1, DRPLA, MJD, SCA2, and SCA6 CAG repeats in 48 Portuguese ataxia families. *Am J Med Genet* 81:134–138.
- Stennicke HR, Salvesen GS (1999) Catalytic properties of the caspases. *Cell Death Differ* 6:1054–1059.
- Sudarsky L, Coutinho P (1995) Machado-Joseph disease. *Clin Neurosci* 3:17–22.
- Sun B, Fan W, Balciunas A, Cooper JK, Bitan G, Steavenson S, Denis PE, Young Y, Adler B, Daugherty L, Manoukian R, Elliott G, Shen W, Talvenheimo J, Teplow DB, Haniu M, Haldankar R, Wypych J, Ross CA, Citron M, Richards WG (2002) Polyglutamine repeat length-dependent proteolysis of huntingtin. *Neurobiol Dis* 11:111–122.
- Tait D, Riccio M, Sittler A, Scherzinger E, Santi S, Ognibene A, Maraldi NM, Lehrach H, Wanker EE (1998) Ataxin-3 is transported into the nucleus and associates with the nuclear matrix. *Hum Mol Genet* 7:991–997.
- Takiyama Y, Sakoe K, Nakano I, Nishizawa M (1997) Machado-Joseph disease: cerebellar ataxia and autonomic dysfunction in a patient with the shortest known expanded allele (56 CAG repeat units) of the MJD1 gene. *Neurology* 49:604–606.
- Trotter Y, Lutz Y, Stevanin G, Imbert G, Devys D, Cancel G, Saudou F, Weber C, David G, Tora L (1995) Polyglutamine expansion as a pathological epitope in Huntington's disease and four dominant cerebellar ataxias. *Nature* 378:403–406.
- Trotter Y, Cancel G, An-Gourfinkel I, Lutz Y, Weber C, Brice A, Hirsch E, Mandel JL (1998) Heterogeneous intracellular localization and expression of ataxin-3. *Neurobiol Dis* 5:335–347.

- Wang G, Ide K, Nukina N, Goto J, Ichikawa Y, Uchida K, Sakamoto T, Kanazawa I (1997) Machado-Joseph disease gene product identified in lymphocytes and brain. *Biochem Biophys Res Commun* 233:476–479.
- Warrick JM, Paulson HL, Gray-Board GL, Bui QT, Fischbeck KH, Pittman RN, Bonini NM (1998) Expanded polyglutamine protein forms nuclear inclusions and causes neural degeneration in *Drosophila*. *Cell* 93:939–949.
- Wellington CL, Ellerby LM, Hackam AS, Margolis RL, Trifiro MA, Singaraja R, McCutcheon K, Salvesen GS, Propp SS, Bromm M, Rowland KJ, Zhang T, Rasper D, Roy S, Thornberry N, Pinsky L, Kakizuka A, Ross CA, Nicholson DW, Bredesen DE, Hayden MR (1998) Caspase cleavage of gene products associated with triplet expansion disorders generates truncated fragments containing the polyglutamine tract. *J Biol Chem* 273:9158–9167.
- Wellington CL, Ellerby LM, Gutekunst CA, Rogers D, Warby S, Graham RK, Loubser O, van Raamsdonk J, Singaraja R, Yang YZ, Gafni J, Bredesen D, Hersch SM, Leavitt BR, Roy S, Nicholson DW, Hayden MR (2002) Caspase cleavage of mutant huntingtin precedes neurodegeneration in Huntington's disease. *J Neurosci* 22:7862–7872.
- Yamada M, Hayashi S, Tsuji S, Takahashi H (2001) Involvement of the cerebral cortex and autonomic ganglia in Machado-Joseph disease. *Acta Neuropathol (Berl)* 101:140–144.
- Yamamoto Y, Hasegawa H, Tanaka K, Kakizuka A (2001) Isolation of neuronal cells with high processing activity for the Machado-Joseph disease protein. *Cell Death Differ* 8:871–873.
- Yoshizawa T, Yamagishi Y, Koseki N, Goto J, Yoshida H, Shibasaki F, Shoji S, Kanazawa I (2000) Cell cycle arrest enhances the in vitro cellular toxicity of the truncated Machado-Joseph disease gene product with an expanded polyglutamine stretch. *Hum Mol Genet* 9:69–78.
- Zhuchenko O, Bailey J, Bonnen P, Ashizawa T, Stockton DW, Amos C, Dobyns WB, Subramony SH, Zoghbi HY, Lee CC (1997) Autosomal dominant cerebellar ataxia (SCA6) associated with small polyglutamine expansions in the alpha 1A-voltage-dependent calcium channel. *Nat Genet* 15:62–69.